CRACK DETECTION IN SOLAR PANEL USING B-NET DEEP LEARNING MODEL

By

BILAL BUTA

NATIONAL UNIVERSITY OF MODERN LANGUAGES

ISLAMABAD

February, 2025

Crack Detection in Solar Panel Using B-Net Deep Learning Model

By

BILAL BUTA

Supervised By

DR. GHULAM MURTAZA

MS Mathematics, National University of Modern Languages, Islamabad, 2025

A THESIS SUBMITTED IN PARTIAL FULFILLMENT OF
THE REQUIREMENTS FOR THE DEGREE OF

MASTER OF SCIENCE

In **Mathematics**

To

DEPARTMENT OF MATHEMATICS
FACULTY OF ENGINEERING & COMPUTING

NATIONAL UNIVERSITY OF MODERN LANGUAGES ISLAMABAD

THESIS AND DEFENSE APPROVAL FORM

The undersigned certify that they have read the following thesis, examined the defense, are satisfied with overall exam performance, and recommend the thesis to the Faculty of Engineering and Computing for acceptance.

Thesis Title: Crack Detection in Solar Panel Using B-Net Deep Learning Model

Submitted By: Bilal Buta **Registration #:** 68 MS/MATH/F22

Master of Science in Mathematics (MS-Math)
Title of the Degree

Mathematics
Name of Discipline

Dr. Ghulam Murtaza
Name of Research Supervisor

Signature of Research Supervisor

Dr. Sadia Riaz
Name of HOD (Math)

Signature of HOD (Math)

Dr. Noman Malik
Name of Dean (FEC)

Signature of Dean (FEC)

February 24th, 2025

AUTHOR'S DECLARATION

I Bilal Buta

Son of Buta Maish

Registration # 68 MS/Math/F22

Discipline Mathematics

Candidate of **Master of Science in Mathematics (MS Math)** at the National University of Modern Languages do hereby declare that the thesis **Crack Detection in Solar Panel Using B-Net Deep Learning Model** submitted by me in partial fulfillment of MS degree, is my original work, and has not been submitted or published earlier. I also solemnly declare that it shall not, in the future, be submitted by me for obtaining any other degree from this or any other university or institution. I also understand that if evidence of plagiarism is found in my thesis/dissertation at any stage, even after the award of a degree, the work may be canceled and the degree revoked.

Signature of Candidate

Bilal Buta
Name of Candidate

24th February, 2025
Date

ABSTRACT

Title: Crack Detection in Solar Panel Using B-Net Deep Learning Model

Renewable energy is seen as an alternative to fossil fuel consumption to reduce environmental pollution. Solar energy is considered the most potential renewable energy source since it is economical and energy-efficient. Photovoltaic panels are susceptible to physical damage which can significantly decrease efficiency and lead to expensive repairs. Conventional methods are laborious and inclined to human error, emphasizing the need for automated systems. In this work, the B-Net model is developed to detect cracks in solar panels. It is based on a convolutional neural network architecture to enhance accuracy and effectiveness in identifying cracks under various lighting and weather conditions. An inclusive dataset containing cracked and non-cracked images of solar panels is employed to enable the B-Net model to learn differentiating features effectively. Findings indicate that the model attains high accuracy and precision in defect detection, better than traditional techniques. Moreover, the B-Net model's performance metrics, such as accuracy, precision, recall, loss, and F1-score, are analyzed to determine its effectiveness. This work contributes to the maintenance of solar systems and prepares the path for further enhancement in automated assessment technologies through deep learning models. The implications of this work extend beyond photovoltaic panel maintenance, offering comprehensive applicability to other fields requiring image-based crack detection.

TABLE OF CONTENTS

LIST OF TABLES

LIST OF FIGURES

LIST OF ABBREVIATIONS

B-Net	-	Bilal Network
CNNs	-	Convolutional Neural Networks
RE	-	Renewable Energy
GHG	-	Greenhouse Gas
N_2O	-	Nitrous Oxide
GMST	-	Global Mean Surface Temperature
GST	-	Global Surface Temperature
ST	-	Surface Temperature
LSAT	-	Land Surface Air Temperature
SST	-	Sea Surface Temperature
U_L	-	Land Components
U_S	-	Marine Components
U_G	-	Global Annual Uncertainty
CO_2	-	Carbon Dioxide
IPPC	-	International Plant Protection Convention
USA	-	United States of America
FC	-	Framework Convention on Climate Change
LED	-	Light Emitting Diode
TWh	-	Terawatts–hours
SRCS	-	Solar Rankine Cycle System
GHE	-	Greenhouse Effect
SD	-	Sustainable Development
SE	-	Solar Energy
Sq.m	-	Per Square Meter
EL	-	Electroluminescence
PV	-	Photovoltaic
2D	-	Two Dimensional
3D	-	Three Dimensional
BC	-	Boundary Condition

PSO	-	Particle Swarm Optimization
FCM	-	Improved Fuzzy C-Mean Clustering
NDT	-	Non-Destructive Techniques
DLIT	-	Dark Lock-in Thermography
ILIT	-	Illuminated Lock-in Thermography
PL	-	Photoluminescence
LIC	-	Quantitative Lock-in Carrier Graphic
AI	-	Artificial Intelligence
NLP	-	Natural Language Processing
SVM	-	Support Vector Machine
RFA	-	Random Forest Algorithm
ELSIS	-	Electroluminescence Smart Inspection System
RNN	-	Recurrent Neural Networks
ANN	-	Artificial Neural Networks
IPA	-	Image Processing Algorithms
ReLU	-	Rectified Linear Unit
TL	-	Transfer Learning
UAS	-	Unmanned Aerial Systems
ITL	-	Inductive Transfer Learning
UTL	-	Unsupervised Transfer Learning
TTL	-	Transductive Transfer Learning
EL	-	Ensemble Learning
Conv		Convolutional Layer
P		Pooling Layer

LIST OF SYMBOLS

C	-	Number of Cracks in Solar Panel
$\Omega(x)$	-	Image Enhancement
$\mu(x)$	-	Number of Neurons
η	-	Number of Convolutional Layers
λ	-	Number of Pooling Layers
$R(x)$	-	Activation function
γ	-	Number of Trainable Parameter
$\xi(x)$	-	Filter Size
$\psi(x)$	-	Number of Weights
£	-	Total Parameter

ACKNOWLEDGMENT

I would like to begin by praising Allah Almighty, who granted me the opportunity to undertake this research and, by His grace, has brought it to completion. I would like to express my deepest gratitude to those who guided and supported me throughout the journey of completing this thesis in convolutional neural networks particularly, in deep learning.

First and foremost, I am immensely grateful to my supervisor, **Dr. Ghulam Murtaza**, for his invaluable guidance, patience, and insight. His expertise and encouragement have been instrumental in shaping my work and in developing my understanding of this complex field. I also extend my heartfelt thanks to my co-supervisor, **Ms. Anab Batool**, for her continual support and constructive feedback. Her knowledge and dedication have greatly enhanced the quality of my research.

Additionally, I am sincerely appreciative of the Head of the Department, **Dr. Sadia Riaz,** the coordinator **Dr. Hadia Triq,** and **Dr. Rizwan** for their unwavering support, insightful advice, and motivation. Their encouragement has been a source of strength throughout this journey. Their assistance and expertise provided me with the additional strength needed to complete this work.

Finally, I thank my family, friends, and colleagues who have offered encouragement and understanding. To all my mentors and supporters, I am forever grateful. This work would not have been possible without their guidance, motivation, and belief in my abilities. For all whom I did not mention but I shall not neglect their significant contribution, thanks for everything.

DEDICATION

I dedicate this work to my friends, family, and teachers, whose encouragement and support are my strength and motivation.

This journey would not have been the same without the unwavering efforts of my beloved

Father

To whom I dedicate this thesis.

"Life doesn't come with an instruction book — that's why we have fathers."

- H. Jackson Browne

CHAPTER 1

INTRODUCTION

1.1 Overview

The inclined dependency on solar energy (SE) has needed the development of effective methods for inspecting and maintaining solar systems. One critical challenge is the extraction of defects, which can variously affect the performance and longevity of solar panels. Recent enhancements in deep learning, specifically convolutional neural networks (CNNs), are crucial in the automated extraction process. The following literature review is focused on traditional methodologies and their applications.

1.2 Background and Motivation

This study is motivated by the urgent need to reduce global warming using renewable energy (RE), particularly solar power. The industry's inclined growth spotlights the importance of maintaining maximum panel performance, which can be minimized due to undetected defects.

1.2.1 Global Warming

Global warming refers to increasing Earth's normal surface temperature due to human acts, mainly releasing greenhouse gases (GHG) from burning fossil fuels and deforestation. The rise of the average temperature of the earth’s surface due to the use of fossil fuels in factories, vehicles, and electricity production is known as global warming. The impact of N_2O (nitrous oxide) was measured yearly from 1900 to 2100, with the help of a global averaged computer model. Nitrous oxide increased to 12.7 TgN/year from 1900 due to fossil fuels and global warming. It was increased temperature by 0.37 °C. To reduce the amount of N_2O in the climate, large cut was required in N_2O [1]. GMST (global mean surface temperature), GST (global surface temperature), ST (surface temperature), LSAT (land surface air temperature), and SST (sea surface temperature) are some of the most important indicators to analyze climate change in the globe. It also explains the uncertainty of climate change using land and marine components.

U_L denotes the yearly uncertainty of the land component and the marine uncertainty is denoted by U_S. Then integrate total global annual uncertainty denoted by U_G. Use formula $(U_G)^2 = (0.29U_L)^2 + (0.71U_S)^2$, where 0.29 is land area and 0.71 is the area covered by water on the globe, respectively [2]. The surface temperature of Earth from 1900 to 2012 was used in [3] and they developed linear regression models that analyze temperature kinetics excluding continuous environmental changes due to human activities and developments. They selected four parts of the earth's surface: the tropical belt, northern, southern, and arctic. The linear regression indicates that with time mean sea surface temperature changes by 0.28 °C in the tropical belt the north of middle altitudes temperatures change by 0.36 °C. The main point in this study is that the warming occurs but not continuously [3]. Global warming due to human being development, industrialization, and other activities is one of the great scientific debates of that time. The study concluded that "global CO_2 emissions must peak and then decline rapidly within the next five to 10 years for the world to have a reasonable chance of avoiding the very worst impacts of climate change" [4]. The authors of [5] explain global warming increases linked to growing human activities and rise in greenhouse gases in the air. The findings in the study [6], describe how global warming increases more rapidly than the International Plant Protection Convention (IPCC) expected due to anthropogenic emissions shown in Figure 1.1. The temperature of the ocean and land both increased in the late 20th century. The expected global warming is 1.7 ± 0.1 °C but the author's results show that it increases by 0.5 ^{O}C more than IPCC's expectation which is 2^{O}C global warming in late 2020, which is twenty years earlier than expected.

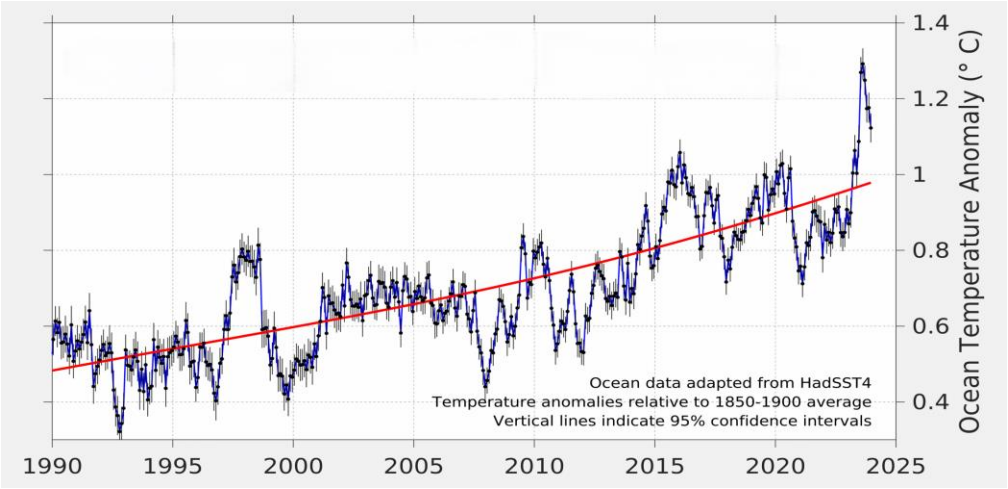

Figure 1.1: Ocean Average Temperature [6]

1.2.2 Importance of Solar Energy

The climate is disturbed due to the continuous different practices of the USA and other countries. These practices threaten ecological and economic costs, as well as social disruption. To overcome this threat, greenhouse gas emissions from burning fossil fuels must be reduced in the coming decades. The solution is based on scientific consensus that led to the Kyoto Protocol and Framework Convention on Climate Change (FCCC). For this USA introduced policies that make sure the changes will not affect the economy. The role of the USA is significant in reducing GHG and CO_2 emissions because it reduces large amounts of these gases. America reduced 14% less than 1900 levels in 2010 and targets downward emissions for climate protection. They decided to adopt more energy-efficient techniques with no or very low carbon reduction. Including transportation that has low fuel consumption, improved infrastructure for alternative transportation modes like biking, walking, and use of local transport instead of own cars. Also rapidly increases the renewable resources [7]. The bestseller book describes, "Drawdown: The Most Comprehensive Plan Ever Proposed to Reverse Global Warming, measures, models, and describes the 80 most substantive existing solutions to address climate change mitigation" describes several solutions at the level of households, individuals, and direct changing patterns of consumptions. Some researchers said that individual actions such as "behavioral wedges" play a significant role in reducing emissions. This book gives three main solutions one of which is to replace current technologies and practices up to 2050. It also gives thirty other actions to reduce emissions some of them for land management are reduced food waste, plant-rich diets, clean cook-stoves, composting, silvo-pasture, tropical staple trees, tree intercropping, farmland restoration, regenerative agriculture, managed grazing, improving rice cultivation, conservation agriculture, nutrient management, farmland irrigation. For transportation are electrical vehicles, ridesharing, mass transit, telepresence, hybrid cars, bicycle infrastructure, walkable cities, and electrical bicycles. For energy and materials, are methane digesters, LED lighting, household water saving, smart thermostats, household recycling and recycled paper, micro-wind, solar water, and rooftop solar. The author said the rooftop solar systems installed in households for providing energy make a great impact on reducing emissions and are estimated to contribute 6.88 percent of total electrical energy worldwide by 2050 which is nearly 3600 terawatts–hours (TWh) [8]. CO_2 can be used as a natural working fluid. It introduced a new concept to tackle global warming and introduced a novel system called

supercritical CO_2 Solar Rankine Cycle System (SRCS) consisting of a mechanical feed pump (thermally driven pump), solar collectors, heat exchangers, and a power generation turbine. The Rankine Cycle consists of flow-regulating elements, an evacuated tube solar collector, a gas & liquid heat exchanger, and turbines. It provides new techniques for future use of green energy resources and gives highly potential solutions [9]. The greenhouse effect (GHE) is stronger as needed and more heat is trapped as compared to heat escaping in space. This is the reason for global warming. These gases affect human beings, animals as well as nature. Due to that different diseases spread like hard to breathe, damaged lungs, irritated nose & eyes, asthma, and heightened sensitivity to allergies. Almost twenty-three million people in the USA suffered from respiratory issues or asthma in 2010. Human infections, dengue fever or break-bone fever, headache, bone and joint aches, rash, malaria, and 130 species of mosquitoes are some other effects and diseases. Climate change also threatens water like flooding, which happens frequently. Extreme weather also badly affects lives. To tackle this world need to increase planting and conserving forests or woodland. Also, sustainable development (SD) is needed like sustainable construction methods, dredging of waterways, efficient waste disposal and recycling methods, landscape architecture, and sustainable energy utilization [10]. Energy insecurity is a major problem for humans in this era. To address it 145 countries developed roadmaps and use technologies that depend on wind, water, and solar energy to 100% transitive by 2035. Also, the target is to use 80% sustainable energy by 2030. The use of hydrogen fuel-cell transportation should increase as compared to battery electric vehicles because it is costlier [11].

1.2.3 Growth of Solar Energy

Due to global warming governments of several countries taking steps including increasing renewable energy sources, improving energy efficiency, and encouraging people to use sustainable resources. Different researchers define SD including Rees (1989), Pearce (1989), and Pezzey et al. (1989). Pezzey said, “SD might require that welfare is above some minimum level and that the growth is ecologically sustainable”. Rees (1989) said that “SD requires ecological diversity and productivity in developing regions”. Adams (1900) said, “SD is intensely synthetic, and the second characteristic is the apparent ease with which different ideas about development are grafted on”. The origin of SD is placed by Barbier in the 1970s. He suggests two standards the first is realizing the value of the “basic needs” approach to helping the

poor and the 2nd is that “real development” is not possible if we ignore the environment. There should be a balance between population growth and SD. Daly (1989), Barbier (1900), and Conway agree that “achieving a stable population is an essential pre-condition for a truly sustainable development” [12]. The researchers review similarities and differences in explaining or defining SD, technical methods, motivation, and process. They find that there are no universally accepted indicators based on compiling theories, influential in policy, analysis, and data collection. It suggests people in different areas should use different terminologies, data, and methods for measurement. They give a framework to enable distinguishing among targets, driving forces, goals, trends, indicators, and policy responses. They also highlight that continued research is necessary on critical limits, scales, aggregations, and thresholds [13]. The concept of sustainable energy development is multi-dimensional and varies in meaning depending on the context it is applied and the user’s perspective. The importance of energy in sustainable development was recognized in 1987. The concept of sustainable energy development became an international agenda when the United Nations set the goal of energy to achieve SD. To get affordable and reliable energy is integral to sustainable development. To reduce harmful effects, it is necessary to transform the current energy system [14]. Figure 1.2 shows the solar installation worldwide.

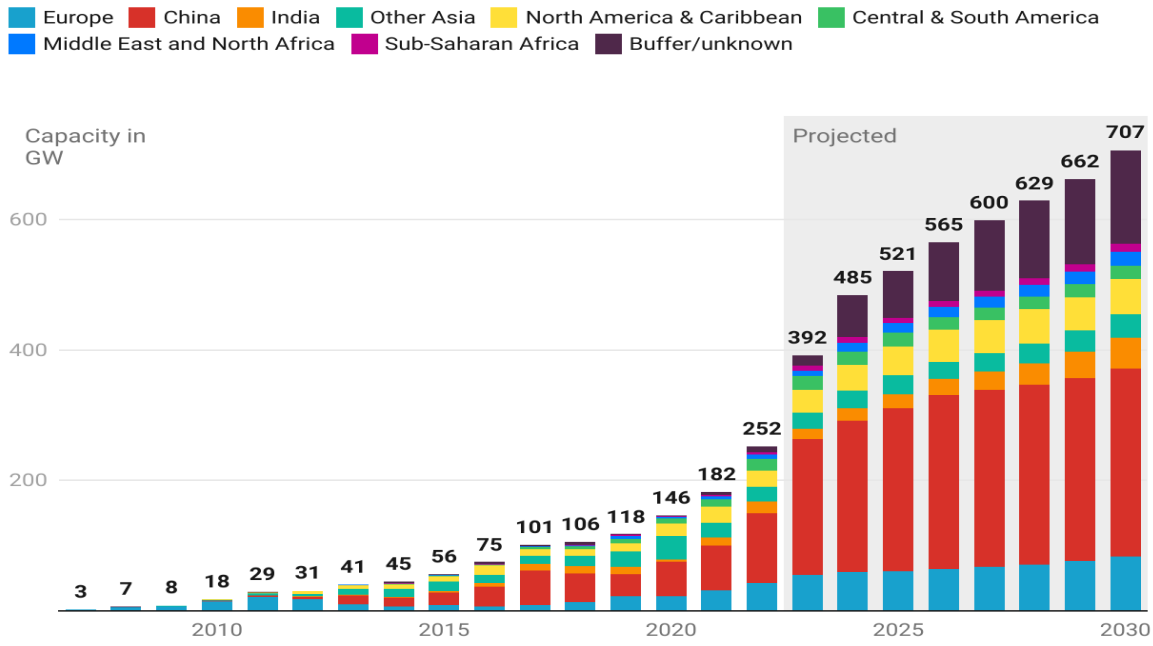

Figure 1.2: Installation of Solar System Worldwide [73]

1.2.4 Significance of Solar Energy and Maintenance for Optimal Performance

Several governments promoted renewable energy resources in households and commercial uses to control climate change due to carbon emissions. One of the most used renewable energy resources is SE which is highly underutilized. The world, Australian continent has an excessive amount of solar radiation per square meter (sq.m) as compared to other continents. This study focuses on how to improve SE systems in Australia, the challenges of installing solar systems, and the benefits of using renewable energy systems. Studies show successfully transferring SE will make sure that it will make a remarkable contribution to electricity generation in Australia and the country will meet the demand for clean energy. Due to technological advancement and the increase in population world needs to generate more energy to fulfill its requirements. The need is to get reliable, everlasting, and cost-effective renewable resources to tackle the rising demand of the future. SE plays a vital role in getting long-term energy production that is freely available and managing concerns in energy crises. The solar industry is growing rapidly all over the world due to the increasing demand for electricity while the other resources are expensive and fossil fuels are limited and not reliable. SE has become a tool to enlarge the economic status of developing nations and develop the lives of numerous common people because it is cost-effective due to long research to advance its development. This energy is the finest option for the upcoming demand for energy and it is worthwhile in terms of capacity, availability, accessibility, and efficiency among other renewable energy resources. This study focuses on barriers to a better solar industry and discusses how to upgrade the solar industry, the world energy scenario, its applications, and fundamental concepts of solar energy to resolve the energy crisis [28]. The depletion of fossil fuels with time and unfavorable environmental effects drive the world toward clear, reliable, and sustainable forms of energy resources. The development to improve the performance of the solar industry has made it one of the best energy resources in the past couple of years. This study measures the threads, strengths, opportunities, and weaknesses of using solar systems. With the technological advancement, the cost of solar systems is also considered to be an opportunity to use it. Although there are some weaknesses and threads that exist to use SE for example energy storage requirements are a challenge, most of the problems are addressed with technology advancement [29]. Suitable maintenance maximizes the energy output and increases the lifespan of solar cells. Timely

repairing and inspection help to address and identify problems/issues before damage and ensure good performance [55].

1.2.5 Challenges in Manual Inspection and the Need for an Automated Crack Detection System

There are various challenges connected with manual inspection methods and techniques that realize the need for automated detection systems to ensure accuracy and efficiency for solar energy production. The methods related to manual inspection are inclined to human error, time-consuming, and labor-intensive. It leads to missed cracks, defects, and inconsistent results. In populated areas, manual inspection faces safety challenges, and it makes it difficult to understand and identify structural issues properly. This type of limitation increases cost and delays the work because inspectors visit sites repeatedly for assessment and to correct errors made during inspection [56, 57].

1.3 Crack Detection in Solar Panel

There are different types of cracks in photovoltaic modules that will be discussed in detail, the impacts of cracks in solar panels are mentioned and previous methods to cracks are exhibited in the below subheadings.

1.3.1 Types of Cracks in Solar Panels

Photovoltaic (PV) modules are especially susceptible to cracks that can seriously affect both the lifespan and the panels' efficiency. These cracks can often be divided into two groups: macro cracks and microcracks. Microcracks are minute fractures, usually measured in millimeters or less, frequently happening during production or due to mechanical stress during setup and use. They could be invisible at first, but they can cause a slow drop in solar cells' electrical conductivity, which lowers their efficiency. Numerous elements, including mechanical loads, heat cycling, and harsh weather like hail or deep snow, can cause these microcracks to form. They are especially dangerous since they may eventually result in more serious problems like hot spots, which can reduce the efficiency and performance of solar modules and potentially cause the failure of cells. On the other side, macrocracks are easy to find due larger size as compared to microcracks and have a significant effect on the performance of modules. Macrocracks derange the electrical pathways in cells. Due to cracks, there are power losses and

failure of modules. These cracks are made due to intense or strong weather conditions, improper handling, and installation errors. Both types of cracks are not good for solar panels leading to a decrease the power output and escalating the cost of maintenance [59]. Several methods are used to identify and extract cracks in solar panels like infrared thermography and electroluminescence (EL) images. It is used to identify microcracks because EL imaging can visualize the electrical pathways and activities of solar modules and can find hidden cracks that are different from to seen with a standard visual inspection [60]. Different types of cracks in solar panels are shown in Figure 1.3.

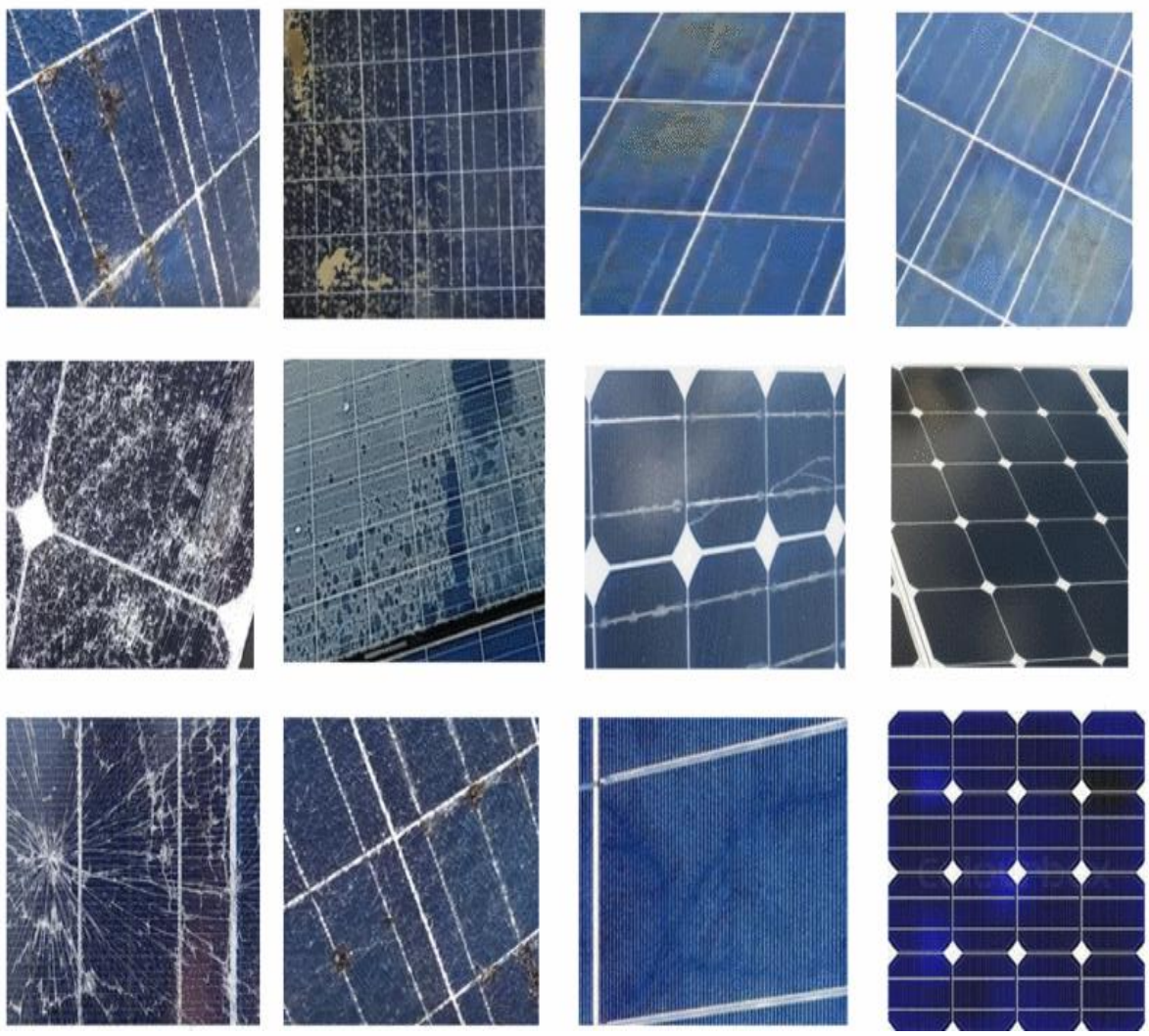

Figure 1.3: Different Cracks in Solar Panel [76]

1.3.2 Impacts of Cracks in Solar Panel Efficiency and Lifespan

The Sun is an illimitable source of energy that can fulfill all the energy requirements of human beings. The direct way to generate electricity from solar energy is by using photovoltaic cells and the indirect way is by using concentrated solar power. The efficiency of cells is nearly 34.1% in multi-junction cells. Concentrated solar technologies are also efficient in generating electricity has a promising future as well because it has energy storage capability and high capacity. The SE is also used in agriculture for irrigation. It has applications to power motor vehicles and other uses like cooking and space heating. The most advanced practicability for the SE is transmitting electrical energy from space to Earth using a satellite power station via microwave beams. The most serious challenge of using SE is that it is unavailable all year due to its high capital cost. This study discusses storage-related, economic, technical, and environmental challenges. Nowadays one of the major technologies is photovoltaic panel installation, worldwide for energy production. Effective cost is one of the reasons for spreading installation of photovoltaic (PV) systems in domestic and industrial use. With the increasing use challenges are also created for manufacturers and customers, especially the quality of photovoltaic cells during service lifetime to withstand environmental conditions. Thus quality of the panels is a crucial aspect. Developing cracks on panels should be considered before installing PV power plants. Due to cracks, there is a chance of loss of energy during the operational phase. There are different cases of these micro-cracks with different shapes, sizes, and orientations [30]. The effect of micro-cracks on PV cells and the loss of energy generation due to micro-cracks are described in [31]. The author uses data taken from several projects in Jordan and explains the effect of micro-cracks on energy loss. Also gives an indicator that identifies what helps someone to decide whether to change a faulty panel or not.

Figure 1.4 contains two graphs (a) and (b), which show the analysis of output power and efficiency of solar cells. They demonstrate the impact of diagonal cracks on solar cell outcomes. Graph (a) illustrates the power output over time, cracks minimize the performance relative to the theoretical maximum. Graph (b) analyzes this reduction in performance as the number of defective cells increases. The analysis with the help of these graphs shows the negative effect of cracks on solar panel performance [72].

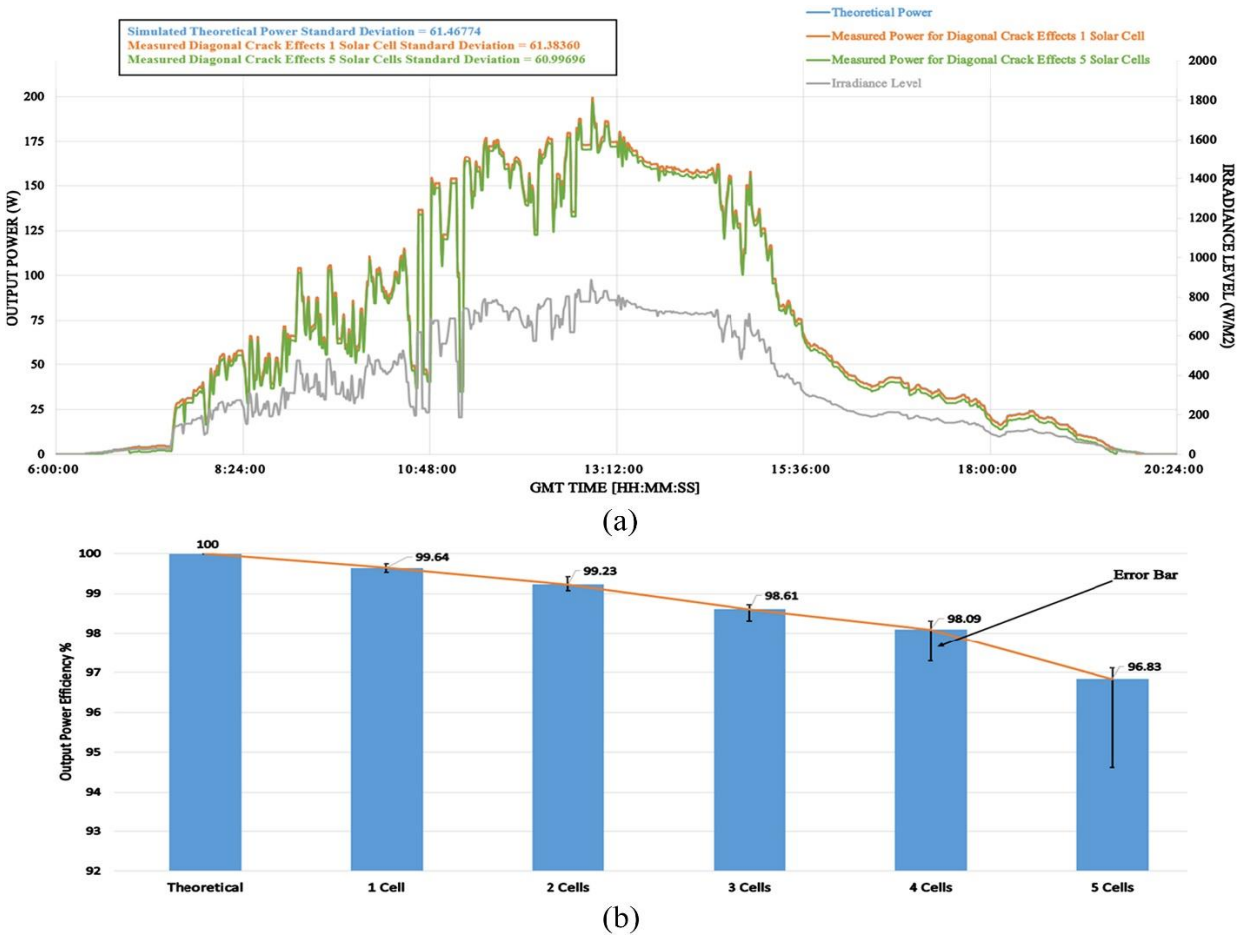

Figure 1.4 Cracks Reduce Efficiency of Panels [72]

1.3.3 Current Methods for Crack Detection on Different Surface Excluding Solar Panels

There are several methods to find cracks on PV panels before discussing cracks, and the different nature (shapes and size) of cracks on panels; we will discuss general methods to find cracks on different surfaces. The authors of [32] use a sampling method to find or identify cracks on 2D / 3D acoustic waveguides. The sampling methods are the factorization method and the linear sampling method. Here model version is used for these sampling methods. It shows if someone deduced or knows the type of boundary condition (BC) that truly applies to the cracks then it is easy to formulate a sampling method for that BC to ensure the effectiveness of the method. With the use of 2D examples, the need for such type of adoption is proved numerically and theoretically. Study shows factorization method is also can be applied in a waveguide with

similar data used in the linear sampling method. The identification of cracks or multi-cracks in beams, the inverse method, and natural frequency-based forward methods are proposed in [33]. The definition of natural frequency drops is simply explained by forward methods. The author uses the local flexibility model of the cracks approach and determines the ratio between natural frequencies from un-crack and multi-crack beams. The non-linear crack effect is not considered in this approach that can be neglected when there are no excessive cracks. Also, they have expressions that can identify the connection between the natural frequency drop and the crack depth. The natural frequency ratio is used to verify the efficiency of these methods, acquired from the finite element package. The natural frequency ratio is also used for validation of the crack detection methodology. The method presented in this study expresses that the depth ratio of cracks and locations is successfully predicted. There are two types of damage to concrete structures: cracks and cavities. They can reduce tightness and lord-bearing of structure that can be failures in construction structure. Uncontrolled or excessive cracks in the structure may weaken the resistance and corrosion. Moreover, structural cracking can badly affect its artistic, and in verse cases it is dangerous for people who live in such buildings [33]. They deeply review the development of damages and the formation of cracks in the structure of concrete surfaces. This study focuses on the characteristics of basic types, the initial cause of cracking, an overview of used methods for detecting the shape cracks or microcracks, and diagnosing. There are eight specific criteria for finding types of cracks on concrete surfaces [34]. To find cracks in highly heated exposure on concrete surfaces local binarization method is used. Using the local binarization algorithm, the greyscale images of a surface cross-section were binarized. Then the isolated cracks were drawn out to examine area, length, and width. The local binarization method uses real images of surfaces of high temperature and cross-section area to examine the effectiveness. Some cracks that were not detected can be found using different parameters [35].

1.3.4 Current Methods for Crack Detection in Solar Panels

The new framework to identify and distinguish cracks on panels is used in [36]. Previous techniques used for crack detection are less efficient with high cost, a lot of computational time, and low precision. Due to these flaws, the author introduces **utilizing optimization techniques** depending on segmentation. In this segmentation process, the cracks have been found and then optimization algorithms were run to discover the crack pixels. This article claims that the method

can find complete cracks with low computational cost and high accuracy. For crack detection on the surface of solar cells, they introduce an automated inspection system ground on an image processing approach. The **Particle Swarm Optimization algorithm** (PSO) is the leading component of his proposed method for the detection of cracks in solar cells. **Fuzzy logic** is also used to find some features, especially bus bars, and cracks, and will classify damaged products and cracks based on the location of bus bars. The given method can give good results based on the PSO, using an automated inspection system. The extraction of cracks is difficult due to the uneven and complex texture background of images of solar panels [37]. The method is proposed that uses a combination of morphologic features and image texture to find cracks. Firstly, the **Laplace pyramid decomposition method** and linear filter are used to suppress the multi-scale details and background texture. Secondly, use the **modulus maximum method** to extract the edges of images. Finally, the **Improved Fuzzy c-Mean clustering (FCM)** was used to extract cracks by a combination of the texture and morphologic features of images. Also, an improved region growth algorithm is used to find reasonable and accurate results for the identification of cracks. It is helpful to promote the use of solar systems in more industries [38]. In the PV system, the most critical component is PV cells. The focal objective of this study is to review the impact of microcracks and cracks on the electrical efficiency of silicon solar cells and list the famous techniques to determine cracks. There are different degradation modes in PV modules like yellowing, delamination, bubbles, cracks in the cell, defects in the anti-reflective coating, and burnt cells. The author checks the behavior of cracks and cells using different tests involving mechanical load tests, strength tests, humidity freeze tests, and thermal cycling tests. This paper describes that during manufacturing various tools are used for defect detection. In this section, **cross-section techniques** and **non-destructive techniques (NDT)** are described. Some NDTs are dark lock-in thermography (DLIT), induction thermography, illuminated lock-in thermography (ILIT), Electroluminescence, photoluminescence (PL), quantitative lock-in carrier graphic (LIC), and some others [39]. The innovative parameter extraction method for different types of solar modules was instituted on the **Adaptive Differential Evolution Technique**. The single-diode model is used for cracks and parameter extraction. The objective function is used to reduce variance (ADET) between measured and estimated values. The results found from the adaptive differential evolution technique are compared with other techniques that are genetic algorithm (GA), organic and inorganic solar cells (OIC), chaos particle swam optimization

(CPSO), and simulated annealing (SA). Lastly, ADPT was validated with different solar modules like polycrystalline, thin film, and mono-crystalline. The proposed method gives satisfactory results. One of the powerful extraction methods is **EL images**, which gives us elevated-resolution images of solar cells. In this paper, 46000 EL images are taken from solar modules with various defects. Using these images, they identify and quantify various types of defects involving series resistant related issues as well as giant recombination regions. They give a method that finds statistical parameters using histograms of solar cell images and employs them as feature descriptors. After that, they trained **Machine Learning (ML) Algorithms** using descriptors [40]. Figure 1.5 shows different fault identification techniques using raw images to find faults on the surfaces.

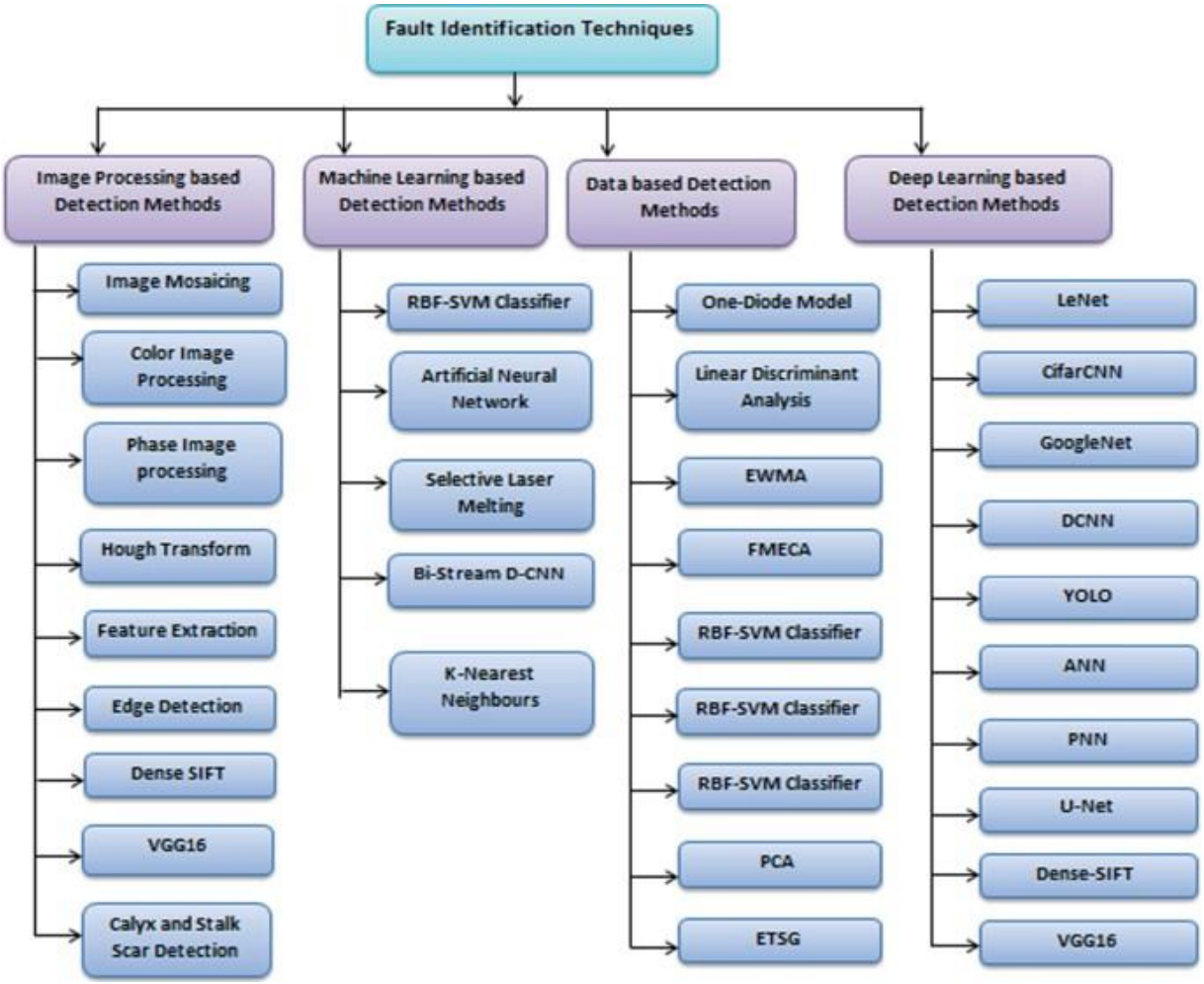

Figure 1.5: Traditional Defect Identification Techniques [41]

1.4 Artificial Intelligence and Crack Detection

Artificial Intelligence (AI) plays a crucial role in different fields, especially in deep learning to inspect and extract cracks in solar panels which are discussed in the following paragraphs.

1.4.1 Artificial Intelligence and Its Applications

AI is a wide-ranging field that is encircled by several methods and techniques that help machines present intelligent behavior. AI has many applications in various domains like manufacturing, finance, transportation, chat-bots, video games, self-driving cars, robotics, education, virtual assistant, healthcare, computer visions, machine learning, market, space exploration, automated grading, customer services, financial services, fraud detection, and google deep mind. One of the best applications of AI is natural language processing (NLP), which helps machines to understand, clarify, and then generate human language. Let's talk about computer vision, it enables machines to recognize and process videos and images like a human. Predicted analysis uses machine learning algorithms to compel predictions depending on data. In robotics, artificial intelligence trains machines to enable automated decision-making and control. Techniques or methods like convolutional neural networks, machine learning, and deep learning are helpful in the advancement of AI applications [61]. Figure 1.6 shows the main branches of AI.

Figure 1.6: Branches of AI [75]

1.4.2 Potential of AI Methods for Automated Crack Detection in solar panel

The AI techniques for automated crack detection in solar panels have acquired remarkable concentration in the last few years. It is observed that solar panels are defense-less against defects and cracks due to several reasons including diverse environmental conditions such as variation in temperature from night to day, wind loadings, freezing, atmospheric pressure load, humidity, manufacturing issues, and transportation. Traditional techniques to find cracks depend on manual inspection and image processing techniques, these methods are time-consuming and make errors. AI approaches have the potential to tackle these shortcomings and limitations by using automated systems and enhancing accuracy.

There are a lot of studies conducted on utilizing AI techniques for crack detection in solar panels. Some of them are Deitsch et al. (2019) introduce a deep learning method for the detection of cracks in solar panels using convolutional neural networks. In 2021, Hu et al. proposed a method for an automated system for crack detection in solar cells using a combination of support vector machines (SVMs) and image processing. These studies are evidence of the potential of automated systems using AI methods to improve accuracy and efficiency for the detection of cracks in solar modules. These techniques are very helpful in the maintenance and control of solar energy systems [62].

1.4.3 Traditional ML Algorithms for Crack Detection in Solar Panel

The solution to the energy crisis is only renewable energy resources because they do not reduce harmful gases that increase the temperature of the world and damage the ozone layer reason of the increasing radiation coming from the sun is harmful to humans. The main renewable energy resource that is used for the production of electricity is solar panel energy. The author uses a deep learning algorithm to classify cracked and non-cracked images. The method provided in it is designed on different modules including pre-processing, amplification, feature computation, crack segmentation, and classification. The dataset is pre-processed with deghost (smoothing) using an adaptive filter and then uses the cumulative enhancement (CE) method to improve pixels of silicon solar module images. Cumulative enhancement computes external features to enhance solar cell images. Then Improved AlexNet (IAN) model classifier is used for

classification with external features. The morphological algorithm plays an important role in segmentation and enables to finding of single and multiple microcracks. It improved the energy production level [42]. ML and image processing are frequently used for detecting faults in solar cells. The old methods cannot give accurate results because the segmentation uses fixed equations and the latter methods learn disordered non-linear features. These features are complex for the human mind to operate. The author employs **Support Vector Machines** for the identification of micro-cracks solar panels. This study proposed an **Image Processing Technique** to instruct the support vector machine model and perform segmentation on electroluminescence images – dataset. This dataset contains 2624 images that are used for classification. This proposed study gives results of 91.079%, 87.289%, 96.314%, and 94.678% for accuracy, precision, recall, and F1 score respectively [43].

Former methods face complexity in EL images and due to limitations in datasets, it is difficult to label faults during the extraction process. To solve this issue, the study proposed a method that combined image processing with an **evolutionary algorithm**, **deep clustering**, **deep learning,** and **transfer learning (TL)** technologies. It can help to label the images according to their faults and defects automatically besides increasing in dataset size. Firstly, the study proposed feature extractor depends on deep learning and classifier for defects. Secondly, use a deep clustering algorithm for the classification of unlabeled defects and keep them separately to upgrade the given dataset lacking any human intervention. Thirdly, TL is used to train the classifier. Finally, the model can identify defects with high accuracy [44]. An automated solar module crack extraction tool based on a convolutional neural network for classification using EL images was introduced. The system is introduced named Electroluminescence Smart Inspection System (ELSIS). The CNNs for ELSIS are based on **InceptionV3 architecture**. This deep-learning model was trained on more than 6000 EL images. This trained model gives 98% results when tested on a large dataset consisting of 3000 images. This ELSIS helps in building satellites with power budgets [45].

An automated system uses EL images that split into cells and detect boundaries of cells using projections on the y and x axes. The regions containing faults are extracted using **Hough Transform** together with mathematical morphology. Cell boundaries are removed carefully then approximately 25 features are determined focusing on statistical characteristics and geometry of

regions of their pixel values. Lastly, using a **Support Vector Machine** and **Random Forest Algorithm** (RFA) features are mapped. The dataset contains 982 EL images taken in the evening light. Here 47244 cells or 753 images were evaluated as faulty. The found results use data in 6 series, with a recall of 0.274 and an accuracy of 0.997 using SVM [46]. The micro-crack detection method based on the ResNet model on multi-crystalline solar cells was developed. To get accurate geometry information, a feature fusion method is created that aggregates strong and low-level features. This technique gives an accuracy of 99.11%. It also trains fault detectors based on MK-MMD using transfer learning. In the past few years, deep learning techniques have opened new directions in the accuracy of learning and detection of useful information from many applications that mainly depend on images like the electroluminescence technique [47]. This work is based on a review of some research paper that depends on deep learning techniques related to the failures in SE in the past couple of years. It also compared hybrid learning and deep learning models and found out some important advantages and disadvantages of each research separately so it provides an overview that helps in the development of this field [48].

The combination of **long-term and short-term deep features methods** for micro-cracks detection is proposed to resolve the problem of poor generality of difficult-designed features. There are two types of ML-based methods, (1) prior knowledge-based method and (2) current viewing knowledge-based method. The ability of these methods is limited and large-scale annotation of images or datasets is inefficient. A stacked denoising auto-encoder is applied to input images to find short-term deep features that represent current information. The prior knowledge is represented by long-term deep features that learn from a huge number of natural images that they see in convolutional neural networks. It concluded that the performance is better in a combination of long-term and short-term deep features as compared to alone. The efficiency of the proposed method is greater in shallow learning-based methods and the proposed method easily finds different kinds of micro cracks [49]. An automated system, the Vesselness algorithm uses EL images of polycrystalline solar cells was adopted. The provided method magnifies crack segmentation; the algorithm gives very fine results in a given database compared to the three approaches. The author shows segmentation code publically it helpful for further research and use as a reference algorithm for polycrystalline solar modules. ML algorithms for cracks are shown in Figure 1.7.

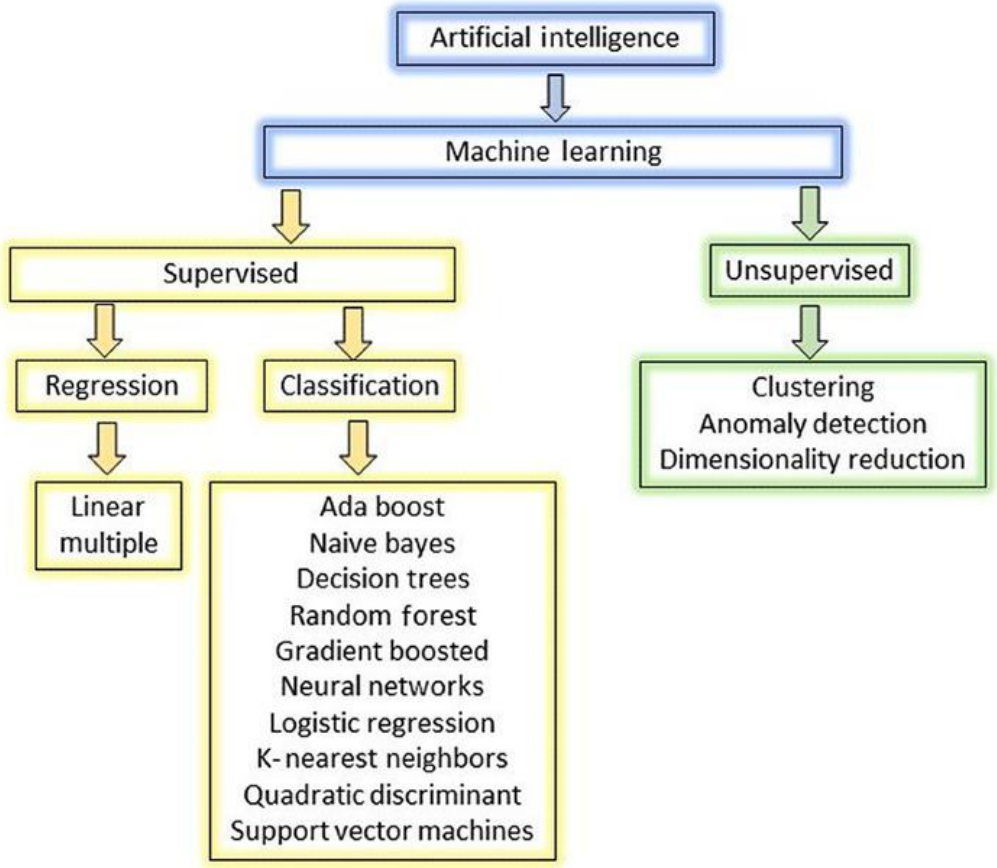

Figure 1.7: ML Algorithms for Crack Detection in Solar Panels [74]

1.4.4 Role of Deep Learning Approach in Crack Detection in Solar Panel

In the recent past, deep learning approaches become encouraging alternatives for automated crack extraction in PV modules. The review of deep learning methods like recurrent neural networks (RNN), artificial neural networks (ANN), CNN, and some others that are used in the extraction of cracks in solar modules. This review discusses the limitations and challenges of traditional methods to find cracks in PV cells. It explores that RNN and CNN are very suitable for image-based tasks for crack detection. The author examines various deep learning algorithms and techniques that have already been proposed for the detection of cracks in solar panels including ensemble methods, single-task learning and multi-task learning approaches, and transfer learning. Also, it discusses datasets that are used in analyzing deep learning algorithms and models. It compared performance together with computational efficiency, sensitivity, accuracy, and specificity of different deep learning models. Finally, it concluded that optimization methods and deep learning architectures are crucial to increase efficiency and

performance. Nowadays silicon solar modules are popular in the market to generate electrical energy from sunlight. The micro-cracks that are inherent in silicon modules can reduce efficiency [51]. The convolutional neural network models to identify and classify microcracks in silicon solar modules are discussed in [52]. The total number of images used was 3951, and they are categorized into different groups, including mono-cracked, poly-corroded, poly-good, mono-good, and poly-cracked. Dense-Net, VGG-16, ResNet50, and VGG-19 are used as pre-trained models of convolutional neural networks for the classification of images where 20% of the data is for testing and 80% is for training. Results show that VGG-19 gives better accuracy as compared to other pre-trained models and overall accuracy is 98.44%. That accuracy is more than the other model. Hence it concluded that VGG-19 is the best option among other pre-trained model for classifying EL images of solar panels. Using this we ensure the better performance of silicon PV modules.

1.4.5 Limitation of Traditional Methods of Image Processing Algorithms for Crack Detection

There are several limitations in traditional methods and conventional image processing algorithms (IPA) for the detection of cracks in solar panels that can slow down their reliability and effectiveness. These methods are based on manual feature extraction and predefined thresholds. These methods are not generalized across various conditions and different types of input images. Also, the performance and efficiency of these algorithms and methods can be remarkably affected by occlusions, noise, misdetections, weather conditions, and lighting variations. In certain algorithms, one of the considerable limitations is the long processing time or huge computational cost. It was found that some algorithms or networks take 16 seconds approximately to find cracks in an image of resolution 6000 x 4000 pixels, which is impractical for real-time applications [63].

Moreover, traditional algorithms or methods struggle and face complex crack patterns that need manual extreme tuning to get sufficient results. These manual preprocessing steps, like filtering and smoothing, can initiate inconsistency and biases in the process of extracting. Additionally, several traditional methods cannot precede new types of materials or cracks. It is limiting their capability in diverse scenarios. Current studies have focused on these challenges and suggest that while conventional methods help extract cracks modern techniques like machine

learning and deep learning can give you outperformed results. These advanced techniques can automatically learn features from images and enhance the accuracy of detection in various conditions [64].

1.5 Convolutional Neural Networks

Convolutional neural networks are a specialized type of deep learning architecture used for images. CNNs consist of fully connected layers, convolutional layers, multiple layers, and pooling layers. When an image is used as input, convolutional layers apply learnable filters that extract features at different scales. Pooling layers are used to shorten the geometrical dimensions of the feature maps. Finally, fully connected layers are used to perform classification based on learnable features [57].

1.5.1 CNN for Image Classification and Segmentation

CNN has a lot of dominance for image classification and segmentation tasks. CNNs are used to detect features of images regardless of image position. Make image features robust/strong enough for translations. The CNN learned features at multiple levels of detachments/distractions from low features including edges and shapes to high-level features including image parts and entire images. The weights used in convolutional filters at different locations, decrease parameters and boost accuracy. There is no need for manual feature engineering for performing classification and segmentation tasks in CNNs [58]. The classification of CNN is shown in Figure 1.8.

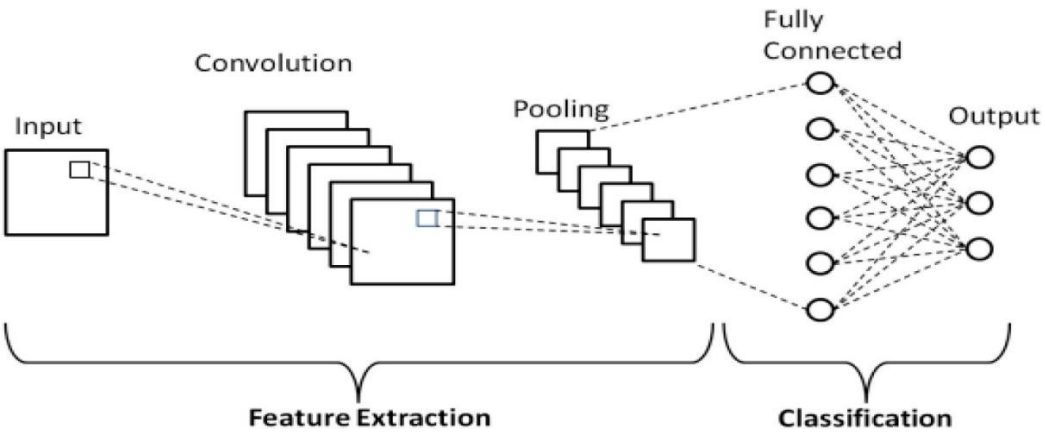

Figure 1.8: CNN for Image Classification [77]

1.5.2 Application of CNN in Various Domains

CNNs used in various domains like image classification, crack detection, semantic segmentation, and medical image analysis. They have achieved ultra-modern performance on standard input image classification data, for example, ImageNet. For object detection tasks they are one of the best options. It can identify multiple objects in an input image. Another area where convolutional neural networks perform significantly is semantic segmentation where they perform pixel-wise classification and give or assign a class label to each pixel in an input image. It also does a great job in medical image analysis. It is used in disease diagnosis, tumor detection, organ segmentation, and various medical imaging tasks. Among these above uses of CNNs, researchers did a lot of work in crack detection based on it. It is used for automatic crack detection in objects and images of infrastructure, roads, and some other concrete structures. It used trained labeled input images of non-crack and cracked areas or surfaces. It can accurately and efficiently identify the location and presence of cracks [57]. Applications of convolutional neural networks are shown in Figure 1.9.

Figure 1.9: Applications of CNN [78]

1.6 CNN-Based Technique for Crack Detection

The CNN is a dominant deep-learning technique for a vast range of applications. It is used in semantic segmentation, image classification, and object detection. This architecture in [53] is created as an automated system to extract features from given raw images and remove the need for physical feature engineering. There are different components in CNN architecture including pooling layers, activation (ReLU) layers, fully connected layers, and convolution layers. In convolutional layers, there are learnable filters applied to input images and find out features together with shapes and edges. The pooling layers decrease the geometrical dimensions of the feature map. The activation function introduced nonlinearity properties. The fully connected layers present high-level reasoning based on identified features. The background of deep learning architectures in [54] started with LeNet (1998), which depends on handwritten digit acknowledgment tasks. In 2012, AlexNet was proposed as a milestone by achieving highly developed results in ImageNet's large-scale visual recognition challenges. When ReLU activation layers and dropouts are used in AlexNet, the benefits of increased network width and depth are demonstrated. After AlexNet different CNN architectures are proposed to increase efficiency and performance. Some of them are ZFNet (2013): to imagine features learned by layers and see the inner workings of CNN, VGGNet (2014) explains that when they increase depth 3x3 filters the performance increases rapidly, GoogleLeNet (2014) allows multi-scale processing in a single network and also introduce inception module. ResNet (2015) uses skip connections to reduce or remove gradient problems in deep neural networks (multiple layers) and it also trains networks with a huge number of layers, DenseNet (2016) creates dense connections in different layers and encourages to reuse of features and also reduces parameters.

The more recent, developers focused on developing more lightweight and efficient CNN architectures that are suitable to insert in different devices, especially in mobile. Some of them are MobileNet (2017) is reduces the cost of computations and several parameters because it uses separable convolutions, Xception (2017) is an extension of architecture named Inception and it uses separable convolutions, ShuffleNet (2017) gives high efficiency because it uses channel shuffling and group convolutions, EfficientNet (2019) can measure resolution, depth, and width because it use compound coefficient, and RegNet (2020) is designing networks for balancing efficiency, performance and proposed by Facebook. These models are marked as milestones for convolutional neural networks in the development of computer innovation. Some techniques

improve the generalization and transparency of CNN like self-supervised learning, attention mechanism, and capsule networks. These architectures achieved significant development in past years. These achievements are due to some innovative ideas including group convolutions, depth, resolution and width scaling, and skip connections. As research continues, it will shape, improve, and luminous the future of architecture [55]. Table 1.1 shows the CNN architectures.

CNN architecture	Year of Lunch	Name of Developer	Improvement
LeNet	1998	Yann LeCun	Convolutional and Pooling Layers
AlexNet	2012	Alex Krizhevsky	Use eight layers, ReLU activation function, and dropouts
ZFNet	2013	Mathew Zelier & Rob Fergus	Improve AlexNet with deeper layers
GoogLeNet (Inception)	2014	Google	Introduce Inception Modules
VGGNet	2014	Oxford	Use 3x3 convolutional filters and 16-19 layers.
ResNet	2015	Kaiming (Microsoft)	Utilize an intense network with 152 layers and introduce residual connection.
DenseNet	2016	Gao Huang	Enhance gradient flow by connecting layers.
Xception	2017	François Chollet	Use separable convolutions to minimize complexity.
MobileNet	2017	Google	It also uses separable convolutions to decrease model size, designed for mobile applications.
EfficientNet	2019	Google AI	Use the compound scaling method
RegNet	2020	Facebook AI	Deploy a systematic design process to make effective architecture.

Table 1.1 CNN Architectures [55]

1.6.1 Limitations and Challenges of the Current CNN-Based Approach

Convolutional neural networks have remarkable performance in crack detection meanwhile several challenges and limitations remain. One of the greatest challenges is the requirement of the huge labeled dataset to train CNN models efficiently. Currently, we have many datasets but they are limited in size and not diverse. Due to this someone faces poor generalization and over-fitting to unknown data. Moreover, these algorithms are computationally intensive. It required sizeable or huge memory and processing power. It can slow down algorithm development in real-time applications. The sensitivity of these networks is another limitation that can variously affect detection accuracy on variations in input data like occlusion, lighting, and noise. Researchers found that models with high results in a controlled environment will not give good accuracy in real-world scenarios, where conditions are unknown or less predictable. A study in [65] explains that traditional neural algorithms struggle to find details about crack patterns. Additionally, the nature of deep learning algorithms makes it difficult to understand how they make decisions. The following table shows the accuracy and trainable number of parameters. Table 1.2 shows the accuracies of the most used CNN architecture using the dataset of [71].

Model(Author)	**Accuracy (Top-1)**	**Number of Parameters**	**Key Features**
Faster R-CNN *(Ren et al.,2015)*	42%	134M	Region-based CNN
Inception-v3 *(Szegedy et al.,2016)*	78.8%	24M	Multi-scale Feature Extraction
DenseNet-264 *(Huang et al.,2017)*	77.9%	34M	Dense Connectivity
NASNet-A *(Zoph et al.,2018))*	82.7%	89M	Utilize normal and reduction cells for scalable image recognition
EfficientNet-B7 *(Tan et al.,2019)*	84.3%	66M	Scalable Architecture

Table 1.2 Accuracies of Some CNN Architectures [71]

1.6.2 Motivation for Developing Novel CNN Architecture for Crack Detection

Due to several limitations of recent CNN-based models, there is a need for developing novel models pointedly modified for crack detection. A new model can address the problems of data scarcity by using techniques like TL. It supports pre-trained models on huge datasets to enhance performance on small-size specific domain datasets. That approach helps improve detection accuracy and precision and decreases the need for huge labeled datasets. Moreover, the novel convolutional neural network merged with advanced and developed pre-processing techniques to improve the quality of the image and reduce lighting diversity the effect of developing an innovative CNN model can increase the trust and use in real-time applications. The new ultra-modern architecture be will more acceptable to practitioners and engineers when the mechanism of the model is easy to understand and explainable allowing predictable decisions. Therefore, these motivations spotlight the potential of improving methodologies of crack detection through novel CNN models that tackle current challenges [65].

1.7 Non-CNN-based Techniques for Crack Detection

There are lots of studies about non-CNN-based techniques for crack detection depending on several traditional image processing methods. These approaches in [66] include tree structures. This model expresses the geometry and topology of crack patterns. Genetic programming is used in image processing algorithms for the automatic generation of images. Image filters like Wiener filters, Gaussian, and median are used for reduction in noise and improvement of crack features. Moreover, the beam-let transform is used as a tool for multi-scale geometric analysis for the detection of cracks. Meanwhile, in unmanned aerial systems (UAS), some cameras are useful for automated inspections. The Shi-Tomasi algorithm also helps in finding corners and helps in extracting crack features [65].

1.7.1 Limitation of Non CNN-Based Methods in Terms of Accuracy and Robustness

There are several limitations in traditional methods, despite their successes, in terms of robustness and accuracy. Achieving high accuracy is one of the big challenges for non-CNN-based techniques. Some other challenges are also characterized such as crack orientations, background noise, and diverse lighting conditions. These techniques are also sensitive to some factors including contrast and image resolution, ruling inefficient performance. Additionally,

traditional techniques tend to be tuned for specific datasets. It is challenging for them to tackle new scenarios [66].

1.7.2 Comparison of CNN-Based and Non CNN-Based Techniques for Crack Detection

The CNNs appear as powerful tools for extracting cracks and give outperformance results as compared to traditional image processing techniques. CNN-based methods exhibit ultra-modern performance, achieving an F1-Scoof re more than 90% in crack extraction tasks. They demonstrate greater validity against background clusters, variation in light, and crack appearance. CNN models with the help of sufficient training data can generalize well to new input datasets in real-world scenarios. Moreover, well-trained CNN models enable quick identification of cracks in real time. However, there are flaws in CNN-based architectures. They need huge datasets for training, which increases computational costs and is time-consuming. Additionally, it is complicated to understand the model's predictions. Also, CNN models needed powerful hardware such as GPUs and significant computational resources [66].

CHAPTER 2

BASIC CONCEPTS AND DEFINITIONS

2.1 Overview

In this context of defect extraction in solar panels, it is necessary to understand the various fundamental concepts and definitions that support the research. This chapter figures out key elements exhibiting a framework for grasping the methodologies deployed.

2.2 Renewable Energy

Renewable energy is energy obtained from natural resources refilled on a human span. There are various natural resources such as biomass, sunlight, geothermal heat, wind, and water. The popular types of renewable energy are wind power, hydropower, and solar energy. Over the last few years, renewable energy become cost-effective and more efficient, and a significant increase in its adoption over all the world [67]. Figure 2.1 shows the types of renewable energy [79].

Figure 2.1: Types of Renewable Energy [79]

2.3 Solar Energy

SE can be defined as the heat and light diffused by the sun that can be controlled using several technologies to generate electricity. There are two main types of SE, passive solar energy; which involves the e direct use of sunlight despite using any mechanical device, and active solar energy which uses technologies such as solar thermal systems and PV systems, to convert sunlight into usable energy [67]. Figure 2.2 shows the production of SE.

Figure 2.2: Solar Energy [80]

2.4 Photovoltaic System

The photovoltaic system is a technology that can convert sunlight into electric current with the help of semiconductor material (silicon). When the light of the sun arrives at the PV cells, it accelerates the electrons, generating electricity. PV systems play a xc significant role in to shift toward renewable resources. It can be used for small-scale (residential) to large-scale (farm) to supply electricity [67]. Figure 2.3 shows the pipeline of SE into electric energy.

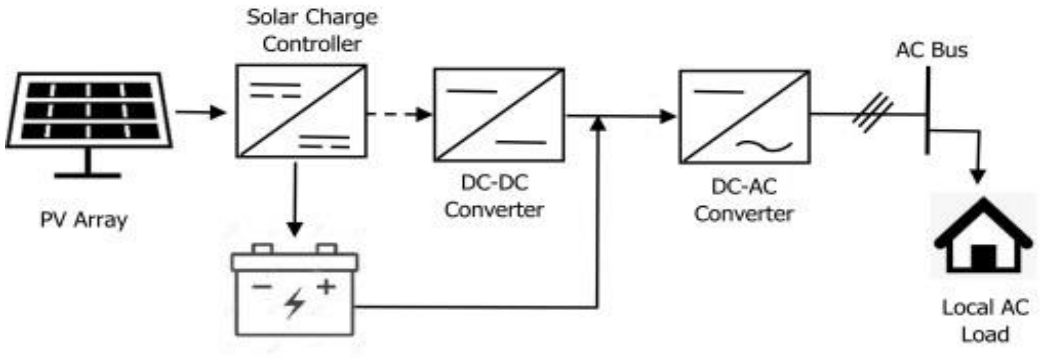

Figure 2.3: PV System [81]

2.5 Cracks in Solar Panel

There are several factors that cracks can occur in solar panels such as thermal stress, manufacturing defects, mechanical impacts, transportation, or environmental conditions. These cracks badly on the performance of solar panels. It is necessary to check and address cracks in solar panels to ensure the efficiency and performance of solar systems [67]. The number of cracks in solar panels is denoted by C.

2.6 Effects of Cracks in Solar Panel

There are various adverse effects of cracks in solar panels, such as increasing the risk of further damage, reducing the lifetime of PV systems, safety risks, and reduced energy outputs. It can disturb the flow of current in the solar panel leading to reduced efficiency and increased operational costs. Moreover, if timely it will not be addressed, it allows or absorbs moisture to enter into the panel which increases the safety risk. Regular maintenance is important for optimal performance [67].

2.7 Image Processing

Image processing is associated with the set of computational techniques employed to examine, enhance, compress, and reconstruct images. It includes transforming images into digital format and executing several algorithms to collect useful information and enhance the visual quality. This process involves various stages: image learning, analysis, manipulation, and output. Image processing is used in several fields including industrial robotics, astronomy, remote sensing, and medicine which makes it important in modern technologies and data analysis [68]. Image processing is shown in Figure 2.4.

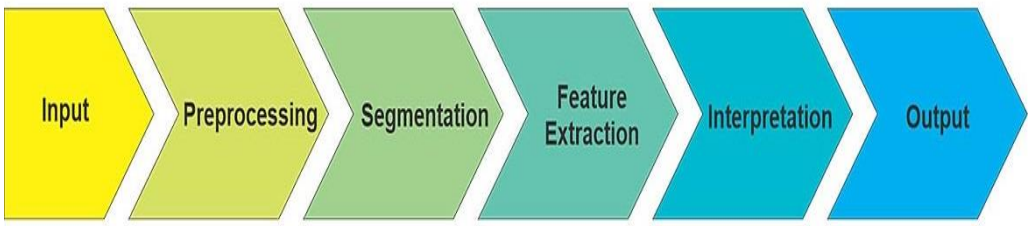

Figure 2.4: Image Processing [82]

2.7.1 Image Enhancement Techniques

It is a method used to elevate the visual appearance of an image that is suitable for analysis. These improvements can significantly enhance the understandability the of image. It has wide applications in satellite photography and medical imaging. Common image enhancement techniques are contrast and adjusting brightness, improving edges to make features clearer, and applying filters to reduce noise [68]. Image enhancement is denoted by Ω(x). Several image enhancements are shown in Figure 2.5.

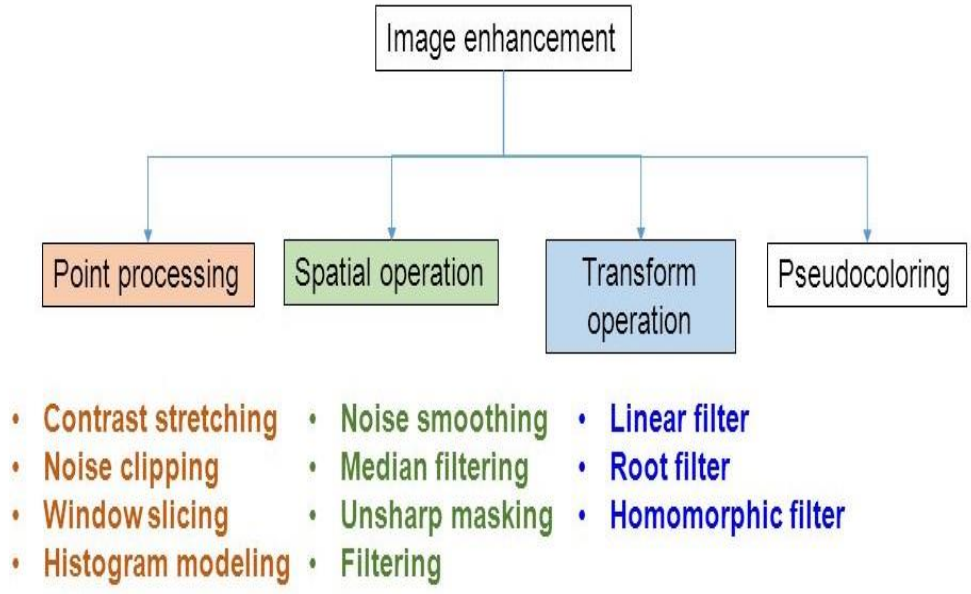

Figure 2.5: Image Enhancement Techniques [83]

2.7.2 Image Representation

This technique involves encoding the visual information contained in the image. This visual information can be analyzed and processed by computers. Image representation particularly includes defining the image as a 2-dimensional array of pixels. Here, each single pixel is referred to as intensity and color. Several representation methods, including RGBA, grayscale, and RGB, provide different types of color information and details, helping in further analysis tasks and processing [68].

2.8 Neural Networks (NNs)

A NN is a computational model motivated by the patterns of biological neural networks in the human brain. It is based on interconnected neurons (nodes) arranged in layers including an input layer, several dense or hidden layers, and an output layer [68]. The number of neurons is denoted by μ(x). General NN is shown in Figure 2.6.

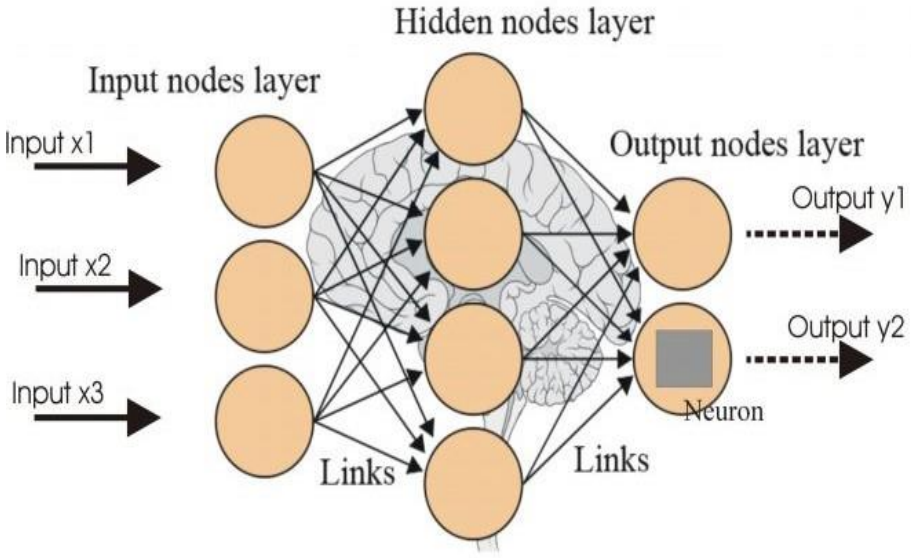

Figure 2.6: Neural Networks [84]

2.9 Convolutional Neural Networks (CNNs)

CNN is a feed-forward neural network that uses filter optimization for feature engineering. It is a category of ML model; particularly CNN which is a type of deep learning algorithm that is quite suitable for inspecting visual data [69].

Application: CNNs are used in image and video recognition, financial time series, recommendation systems, brain-computer interference, image classification, natural language processing, image segmentation, and medical images.

Architecture: It creates feature maps by using filters or share-weight convolution kernels. These filters slide along input features to produce translation-equivariant responses.

Inspection: Convolutional neural networks are inspired by biological processes. It is similar to the connectivity patterns in the human brain's visual cortex.

Pre-Processing: It is commonly used to prepare input data in computer vision. Pre-processing is directly influencing the outcome or performance of ML models.

Overfitting: Regularization techniques such as skipped connections, weight decay, dropouts, etc., help prevent overfitting by discipline parameters in the training of models [68]. Figure 2.7 shows the CNN architecture [69].

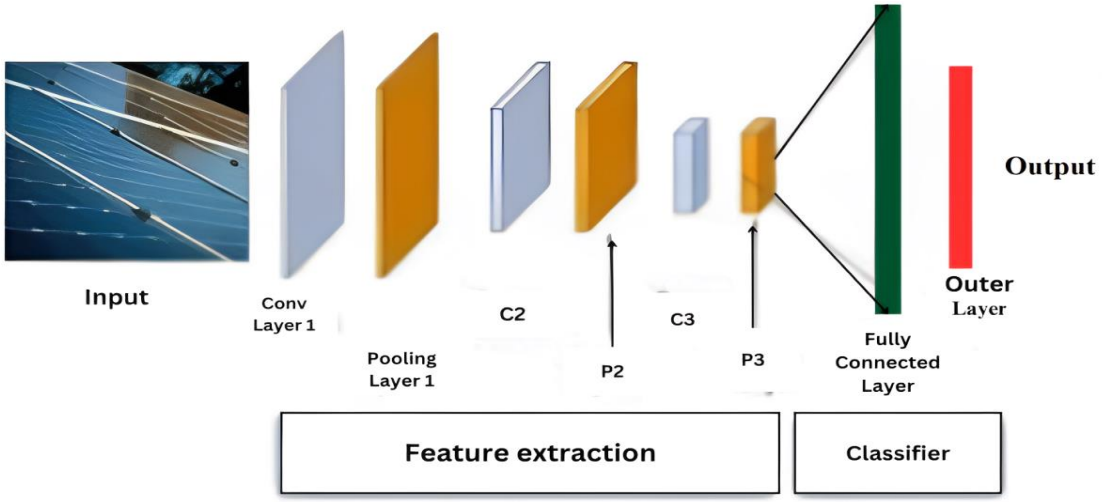

Figure 2.7: CNN Architecture [85]

2.10 Key Components of Convolutional Neural Networks

The key components of CNNs depend on several layers such as convolutional, dense, pooling, dropout, activation, and fully connected layers.

2.10.1 Convolutional Layer

It is a fundamental building block in convolutional neural networks. Convolutional layers are based on a set of learnable filters that have small responsive fields despite that they extend to the full depth of the input image. These filters are convolved over the height and width of the input volume when the input image is forward pass. It computes the dot product of the input and entire filters at any position during the forward pass and constructs two-dimensional activation maps of those filters. This network acquires information from filters that are activated when they extract any specific type of feature from any position of the input [69]. The number of convolutional layers is denoted by η. Figure 2.8 shows the convolutional layer.

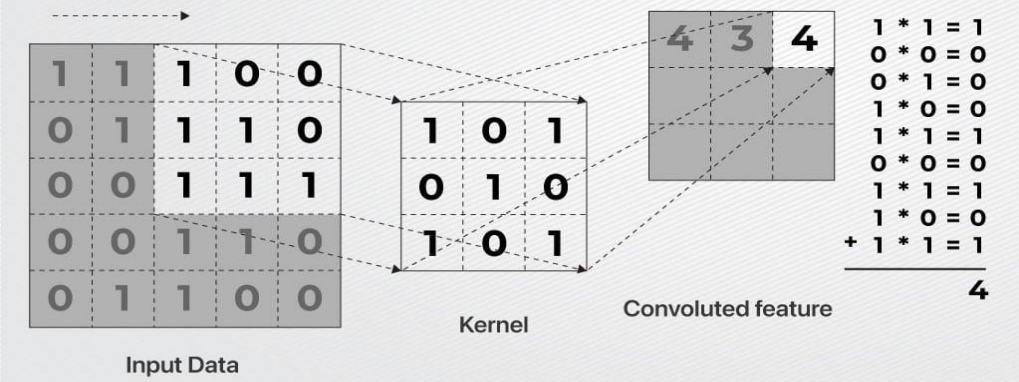

Figure 2.8: Convolutional Layer [78]

2.10.2 Pooling Layer

Pooling layers carry out filtering operations along width and height dimensions and reduce the volume of the input image. There are different types of pooling such as max pooling, global max pooling, average pooling, and global average pooling. Max pooling provides the maximum value of output and it converts input image into parts or sets of non-overlapping rectangles. The pooling layers introduce translation invariance to the network [69]. It is denoted by λ. Figure 2.9 shows the extraction in the pooling layer.

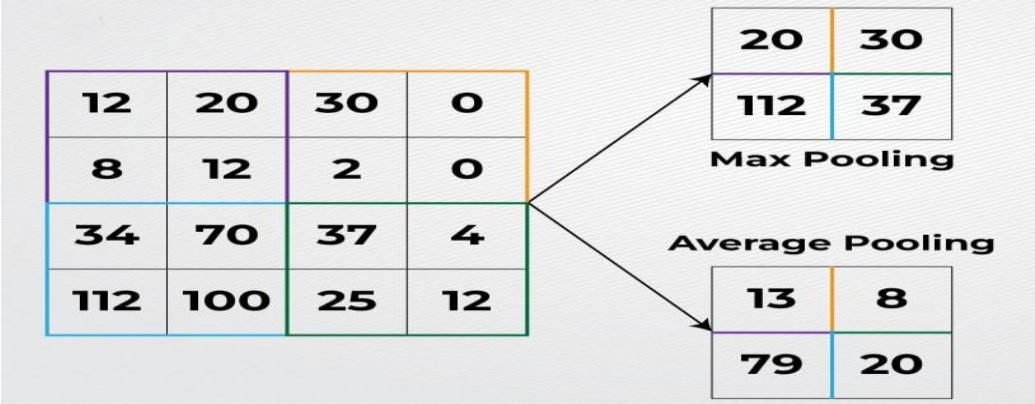

Figure 2.9: Extraction in Pooling Layer [78]

2.10.3 Fully Connected Layer

Fully connected layers, connect layer in the network. It connects every neuron in one layer to every neuron in another layer. CNN works as a traditional multilayer perceptron that

uses features for the classification of input images into different classes [69]. Fully connected layers are shown in Figure 2.10.

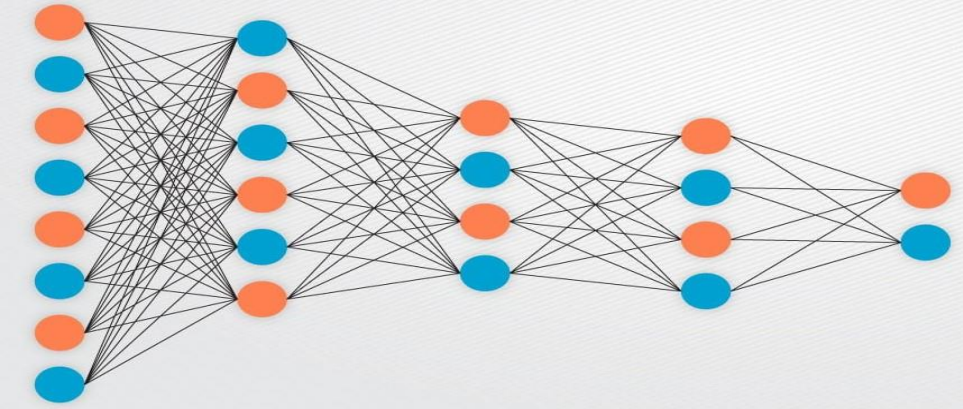

Figure 2.10: Fully Connected Layers [78]

2.10.4 Dropout Layer

The dropout layer is used to avoid overfitting by randomly deactivating an area of inputs at the time of each training update. This pushes the network to learn more features that are helpful in conjunction [69]. Figure 2.11 shows the dropout on hidden layer.

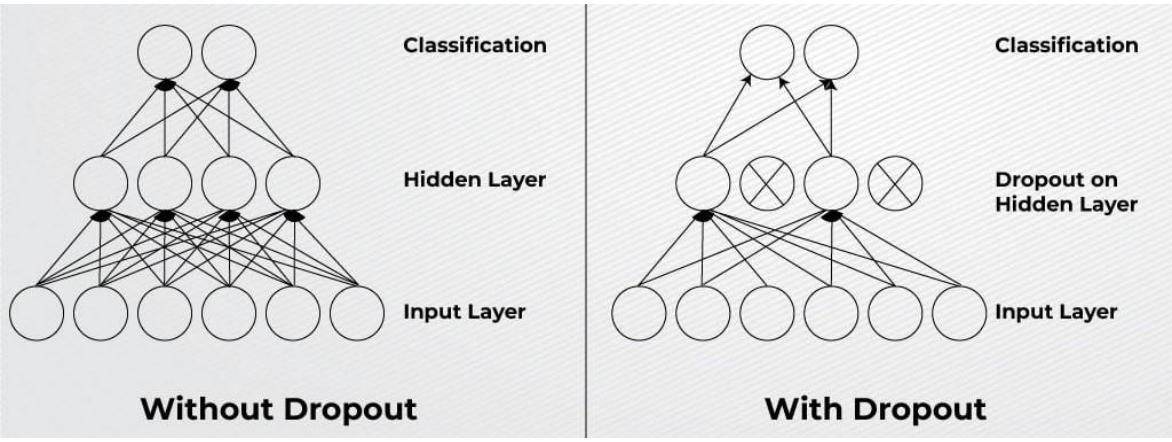

Figure 2.11: Dropout on Hidden Layer [69]

2.10.5 Batch Normalization Layer

To enhance the stability and performance of the neural networks, a technique is used called batch normalization. It normalizes the inputs to each layer. The batch normalization layer

reduces training time, provides higher learning rates, and the network becomes more robust to initialization [69].

2.10.6 Activation Layer (ReLU)

It applies an element-wise activation function. The example activation layer is the $\max(0, x)$ rectifier function also called rectified linear unit (ReLU). It used to be located after fully connected and convolutional layers and denoted by R(x) [69].

2.11 Key Concepts in CNNs

The key concepts in CNNs involve feature mapping, stride, and padding. These are crucial for understanding how convolutional neural networks operate and how CNN transforms input data into meaningful outputs [54].

2.11.1 Feature Mapping

It refers to applying convolutional kernels (filters) to input data that helps the mod extract specific patterns (features) in data. Each single filter is developed to capture particular characteristics including texture and edges, by executing a dot product between the input data and the filter at several dimensional locations. Feature maps are important because they enable the model to learn and understand the hierarchical representation of input data [54].

2.11.2 Stride and Padding

Stride is associated with several pixels in filters by which it moves across the input data. A stride means a filter moves one or two pixels simultaneously. By adjusting the stride, it affects the size of the feature map. The larger strides provide a smaller feature map in the convolutional process.

Padding includes additional pixels across the input data before executing convolutional operations. This is proceeded to control the structural dimensions of output (feature map). Padding ensures that essential features are not lost a maintained in the dimensionality of output [69]. Figure 2.12 shows the stride and feature mapping.

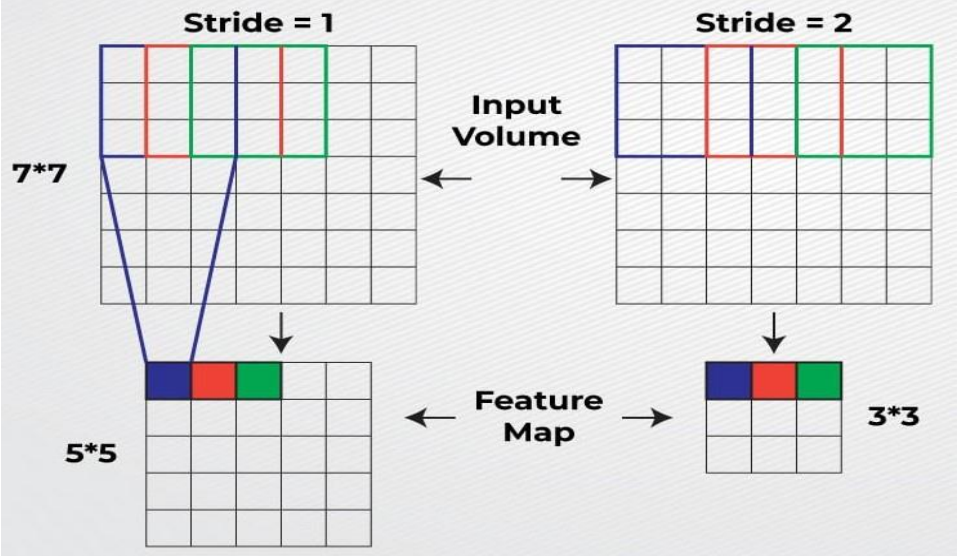

Figure 2.12: Stride and Feature Map [78]

2.11.3 Trainable Parameters

Trainable parameters consist of weights and biases. It is associated with convolutional layers and fully connected layers. To reduce the loss function, trainable parameters are adjusted while training of model. They enable the model to learn from the data [69]. The number of trainable parameters is denoted by γ.

2.11.4 Types of Trainable Parameters

Biases: There are several filters in convolutional layers. In each filter, there is a bias term. This attaches an additional parameter for each filter, which helps the model fit the data better. Weights: In the convolutional layer (conv), each filter has some weights that are learned at the time of training. The number of weights is found by the size of the filter and the number of input channels [69]. Consider if conv has a filter of size 4×4, denoted by $\xi(x)$, and receives input from a layer with 4 channels then the number of weights, denoted by $\psi(x)$, for one filter should be:

$$4 \times 4 \times 4 = 64$$

2.11.5 Calculation of Trainable Parameters

Total trainable parameters can be calculated using the formula:

$$Total\ Parameters = (filter\ height \times filter\ width \times number\ of\ input\ channels + 1)$$

Where +1 takes the bias term for each filter [69].

For example, a convolutional layer has:

$$Input\ channels = 3\ (RGB\ images)$$

$$Number\ of\ filters = 2$$

$$Filter\ size = 3 \times 3$$

Then

$$Total\ Parameters = (3 \times 3 \times 3 + 1) \times 2 = 27 + 1 = 28$$

Where total parameters are denoted by £.

2.12 Famous CNN Architectures

CNN architectures have spread significantly since their foundation, to increase performance on difficult tasks. Some of the famous CNN architectures are given below:

2.12.1 AlexNet

In 2012, Alex Krizhevsky, Ilya Sutskever, and Geoffrey Hiwere developed "AlexNet" in the field of computer vision. AlexNet remarkably outperformed other models in the ImageNet Large Scale Visual Recognition Challenge (ILSVRC-2012) competition. It acquired top-5 error rate of 15.3%. AlexNet used overlapping pooling, ReLU activation function, and dropouts to reduce overfitting [54]. The architecture of AlexNet is shown in Figure 2.12.

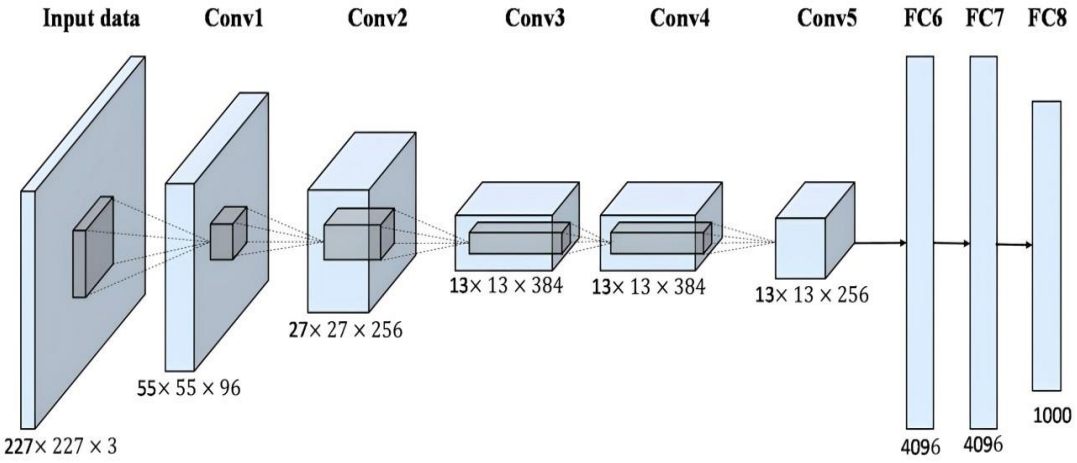

Figure 2.13: Architecture of AlexNet [86]

2.12.2 Improved AlexNet

The researchers continue to enhance the AlexNet architecture, after its remarkable performance and introduced Improved AlexNet. In this architecture researcher used batch normalization which is helpful to accelerate the training process and enhance the performance. This version is also called "AlexNet with Batch Normalization" [54]. The architecture of the improved AlexNet is shown in Figure 2.14.

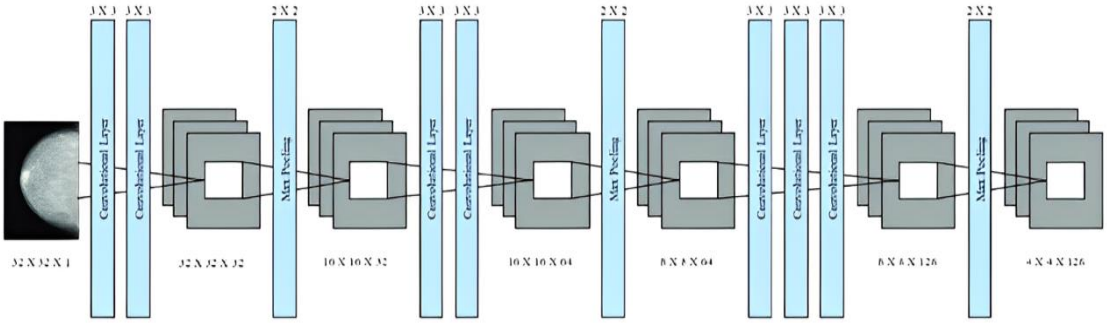

Figure 2.14: Architecture of Improved AlexNet [87]

2.12.3 VGG19

In 2014, VGG19 architecture was developed by Karen Simonyan and Andrew Zisserman. It is developed with 19 layers which exhibit the importance of depth that helps to achieve good performance. VGG19 architecture used 2x2 pooling and 3x3 convolutions throughout the network. In the ILSVRC 2014 competition, it achieved a top-5 error rate of 7.5% [54]. The architecture of VGG19 is shown in Figure 2.15.

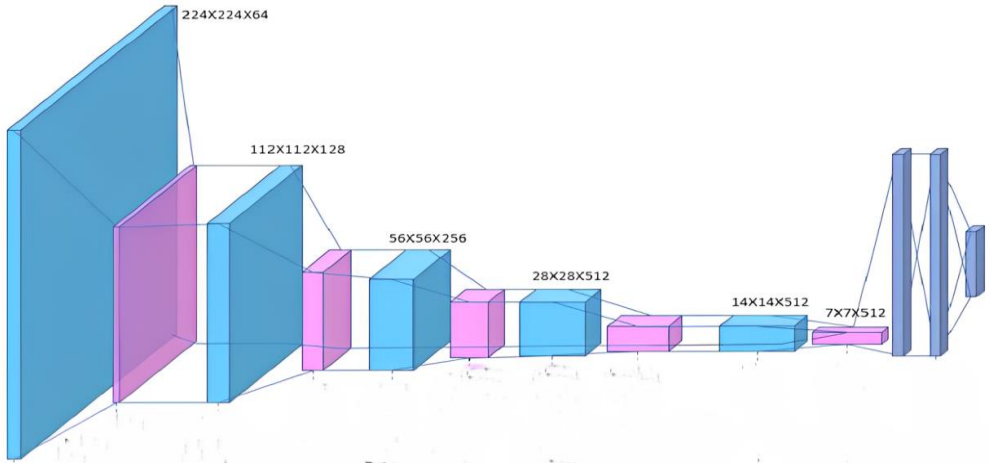

Figure 2.15: Architecture of VGG19 [88]

2.12.4 ResNet50

In 2015, ResNet50 was developed by Kaimin He et al. It won the ILSVRC 2015 with a 50-layer Residual Network. In ResNet50 there is extensive use of batch normalization and featured with special skip connections. It is one of the modern CN models and is widely used by researchers [54]. Figure 2.16 shows the architecture of ResNet50.

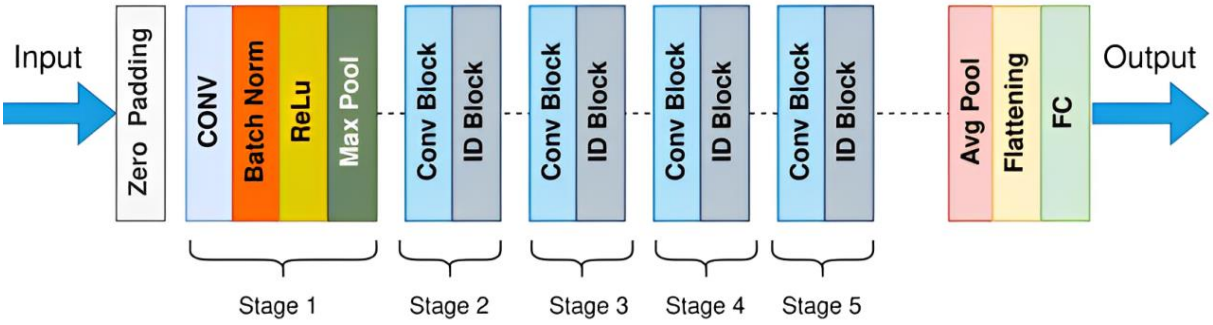

Figure 2.16: Architecture of ResNet50 [89]

2.13 Transfer Learning

It is an ML technique, in it a model trained on one task can be reused for other tasks. This technique enables the model to become a master of the r new tasks based on its previous knowledge and also allows a training model despite having limited data. In TL several approaches are used by researchers on their requirements, these approaches are inductive transfer learning (ITL), unsupervised transfer learning (UTL), and transductive transfer learning (TTL) [70]. Transfer learning is shown in Figure 2.17.

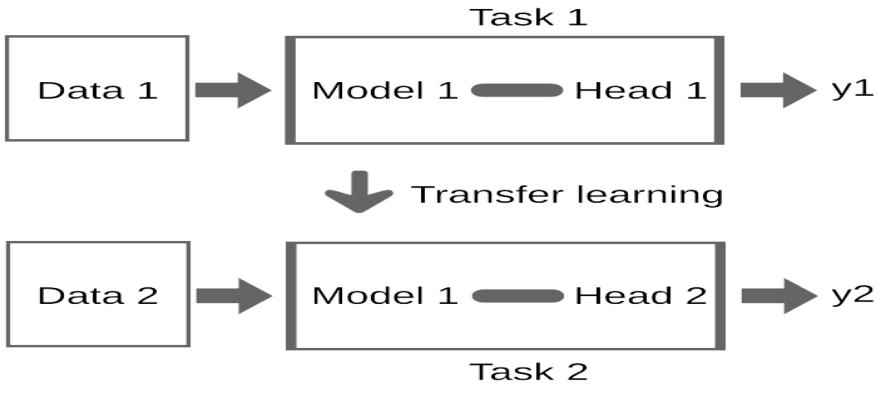

Figure 2.17: Transfer Learning [90]

2.14 Accuracy

Accuracy is a metric that measures the portion of correct/exact predictions made by the model over the whole dataset. Accuracy is calculated as the ratio of the sum of true negatives (TN) and true positives (TP) to the total number of samples. Accuracy is useful but sometimes it misleads when classes are imbalanced. The formula for accuracy is given below [90]:

$$Accuracy = \frac{Number\ of\ Correct\ Predictions}{Total\ Number\ of\ Predictions} \quad (1)$$

2.15 Precision

The precision is defined as the ratio of true positives to the sum of false positives (FP) and true positives (TP). When precision is high it indicates that a model has low FP rates. It is important in situations where the cost of FP is high. It identifies the accuracy of positive predictions of the model [90].

$$Precision = \frac{True\ Positives}{True\ Positives + False\ Positives} \quad (2)$$

2.16 Recall

It measures the ability of the model to find all relevant positive instances. The recall is also known as true positive rate or sensitivity. Recall is calculated as a ratio of TP to the sum of FN and TP. When recall is high it indicates the model is good at capturing actual positive cases [90].

$$Recall = \frac{True\ Positives}{True\ Positives + False\ Negitives} \quad (3)$$

2.17 F1-Score

F1-Score is also known as F-measure. It is a performance metric for estimating the effectiveness of binary classification models. F1-score is crucial in scenarios where the class is imbalanced. When the F1-score is high it indicates that the performance of the model is good [90].

$$F1 - score = 2 \times \frac{Precision \times Recall}{Precision + Recall} \quad (4)$$

CHAPTER 3

FAULT DETECTION AND COMPUTATION OF POWER IN PV CELLS USING DEEP-LEARNING

3.1 Overview

The authors of the review work [91] use a novel approach for finding and extracting faults in PV modules. This paper addresses the crucial issue of cracks or fault detection in solar panel modules. These faults can significantly impact the reliability and efficiency of PV cells. The effects of cracks and faults are various like reduced performance, reduced lifespan of the solar system, damaged connections or wires, danger of fire hazards, and risk of injuries from broken glass. The review work used four different models such as U-Net, Attention U-Net, LinkNet, and Feature Pyramid Network (FPN) to identify cracks in PV cells. Also, ensemble learning is used to combine the results of these four models for improved accuracy. The authors of this paper aim to improve the extraction of various faults including deep cracks and microcracks, using deep learning techniques. The workflow is shown in Figure 3.1 [91].

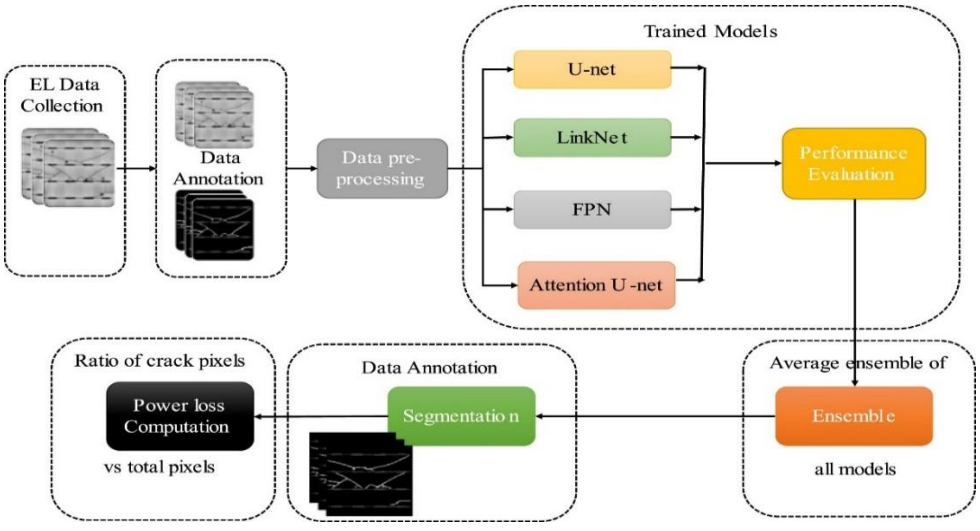

Figure 3.1: Workflow of Review Work [91]

3.2 Key Contributions

The key contributions of Sohail et al. (2023) are focused on the application and understanding of DL methodology, how cracks impact output, and the use of ensemble learning.

3.2.1 Deep Learning Methodology

The authors provide a sufficient deep-learning framework for extracting several types of cracks on PV cells. It involves distinguishing between deep cracks and microcracks that are essential for assessing the structural integrity of PV solar cells.

3.2.2 Impact on Power Output

The researcher interrogates how these cracks affect the power output of solar modules. They spotlight the existence of faults that lead to a reduction in the performance and efficiency of solar systems. It also highlights the need to extract cracks timely to maintain the longevity and performance of PV cells.

3.2.3 Model Evaluation

They employed several deep learning models, like convolutional neural networks (CNN), to distinguish the types of faults based on EL images of solar cells. The models used are evaluated using metrics such as F1-score and accuracy to ensure good performance.

3.3 Methodology

The methodology outlines the techniques and steps used in this work, such as data collection, model training, loss function, ensemble learning, performance metrics, and power analysis.

3.3.1 Data Collection

EL images were used to train the four deep-learning models. The dataset is based on images of solar cells with different types of cracks such as deep cracks and microcracks. These images are used as ground truth for testing and training of models. This dataset is complex for training the models to understand and distinguish cracks effectively.

3.3.2 Model Training

The authors tested different architectures such as U-Net, Attention U-Net, Feature Pyramid Networks (FPN), and LinkNet model, to find out the most effective model for crack extraction in solar modules. These selected models are giving effective results in image segmentation and classification tasks. Standard techniques are used in training these deep learning models including gradient descent and backpropagation. Hyperparameter tuning and data augmentation techniques are also used to optimize models for crack classification accuracy.

3.3.3 Loss Functions

The loss function optimizes the model and produces improved segmentation results. This work used different loss functions on trained models and selected the best result. Two loss functions used in the study are categorical Cross-Entropy loss function and focal loss function mathematically mentioned below:

$$Categorical\ Cross - Entropy\ Loss = -\sum_{i=1}^{n} a_i \log \frac{e^{s_p}}{\sum_i^n e^{s_p}} \tag{5}$$

$$Focal\ Loss = -\propto_t (1 - P_t)^{\gamma} \log p_t \tag{6}$$

3.3.4 Ensemble Learning (EL)

An ensemble learning approach is used to integrate the results of these four deep learning models. EL aims to enhance the overall accuracy of fault classification as compared to individual models. The author implements the weight average ensemble method to strengthen the mIoU of these four models. The outcome of these four trained models is gathered as:

$$y = \frac{w_u \times f_u + w_l \times f_l + w_f \times f_f + w_{Au} \times f_{Au}}{w_u + w_l + w_f + w_{Au}} \tag{7}$$

Where w_{Au}, w_f, w_l, and w_u represent weights of attention U-Net, FPN, LinkNet, and U-Net. The value of weights for models are $w_{Au} = 0.5$, $w_f = 0.1$, $w_l = 0.1$, and $w_u = 0.3$. Here f_{Au}, f_f, f_l, and f_u are predictions of models. y represents the final prediction.

3.3.5 Performance Metrics

These CNN models are evaluated depending on their ability to accurately and effectively detect faults and predict performance degradation. Also, determine a comprehensive view of their effectiveness. The performance of the ensemble approach and models is evaluated using different metrics such as F1-score. The performance metrics and plots are shown in Table 3.1 and Figure 3.2 respectively.

Accuracy	Precision	Recall	F1-Score	mIoU
97.96%	97.95%	97.92%	58.33%	54.19%

Table 3.1 Performance Metrics of Base Paper

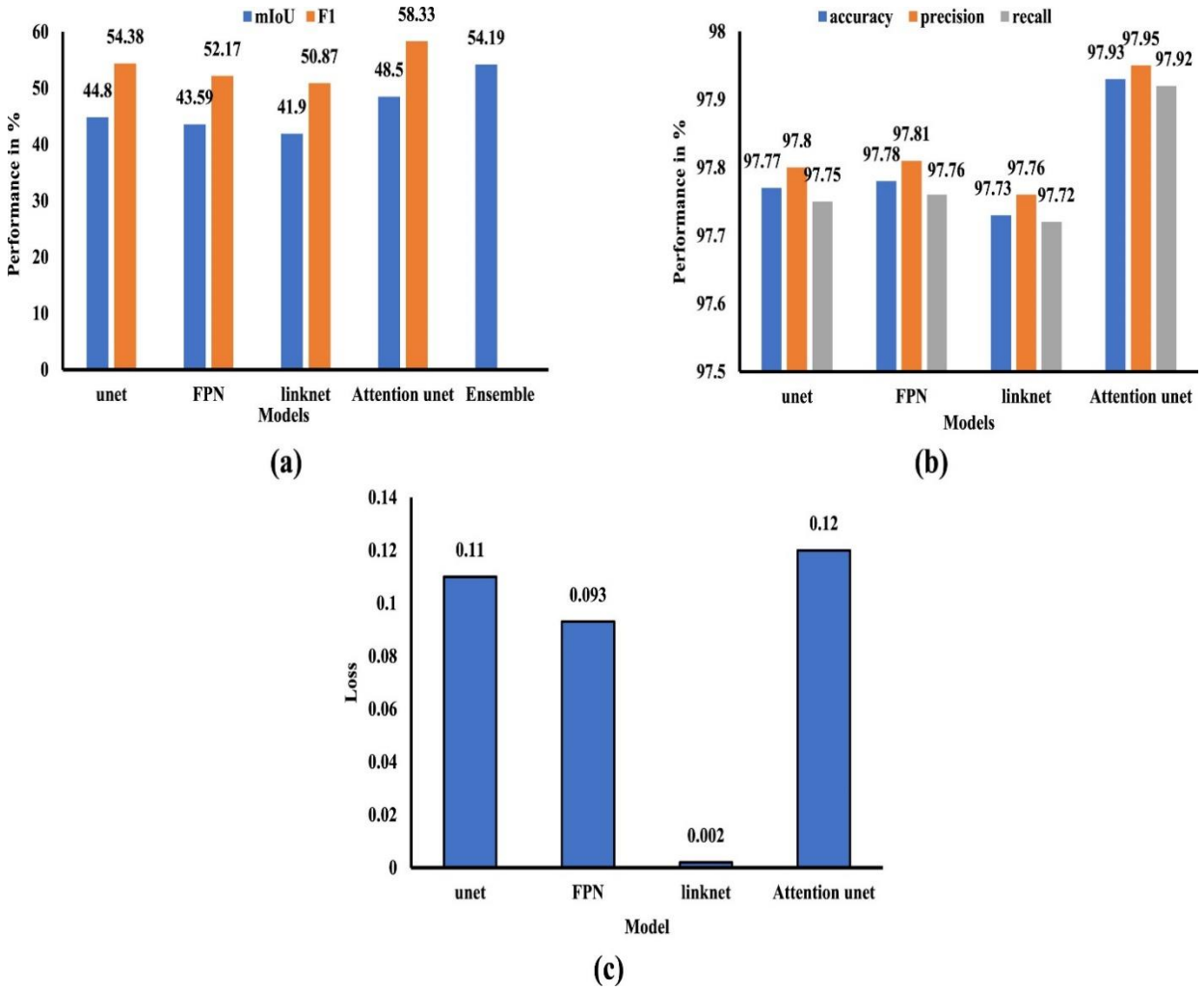

Figure 3.2: Performance of Review Work

3.3.6 Power Analysis

This research not only works on crack classification; it also investigates the effect of cracks on the power output capability of solar modules. In addition, it analyzes the relationship between power degradation and crack size of PV cells. It found that larger deep cracks can lose more power as compared to smaller cracks.

3.4 Key Finding

This section summarizes the key findings, particularly focusing on three areas: fault identification from images of solar panels, power efficiency to analyze the impact of faults, and ensemble learning to combine the different ML models and enhance the performance of the model.

3.4.1 Fault identification

The models used in the study effectively extract and classify various types of cracks in solar cells such as deep cracks and microcracks. The models are trained on a dataset of electroluminescence images and show high accuracy in extracting cracks. These models can classify between microcracks hardness and orientation. It provides a detailed analysis of the structural integrity of the solar modules. This level of crack identification is important for understanding the impact of faults and cracks on power generation and overall solar system performance.

3.4.2 Power Efficiency Analysis

In the base paper, the key finding is that the power generation efficiency is inversely related to the severity of cracks in solar cells. It reveals that deep and larger cracks are directly proportional to power losses. By assessing the relationship between power degradation and crack size, the study provides significant insights into the effects of cracks on solar system performance. This analysis can guide maintenance strategies and also help to optimize power generation output under defective conditions.

3.4.3 Enhancement Using EL

This research discusses the potential of employing ensemble learning techniques to enhance the accuracy of crack detection in solar cells. The ensemble learning approach combines

the predictions of four deep learning models including U-Net, Attention U-Net, LinkNet, and FPN, and outperforms as compared to individual models in distinguishing crack types. The EL approach leverages the strengths of several architectures to develop a more reliable crack detection system. It enhanced the performance and efficiency of solar panel monitoring systems.

3.5 Summary

The detections and outcomes of this paper highlight the importance of deep learning techniques for the worthwhile monitoring and maintenance of solar systems. By enhancing the crack detection capabilities, this method can help improve the efficiency and reliability of PV systems. This base paper provides us comprehensive understanding, contributions, and significance of deep learning models in the fields of fault extraction in PV system and renewable energy.

The base paper shows a comprehensive methodology by applying an ensemble technique, a combination of four deep learning models, and power generation analysis, for detecting cracks in solar panels. It also assesses the impact on solar system performance. The performance metric and dataset depending on EL images ensure the reliability and robustness of this approach.

In this article, there are some limitations firstly, the authors use four different models and then use the ensemble method to enhance the result. It takes more time and increases the computational cost. Secondly, four models train a large number of hyper-parameters as compared to a single model. It makes the process of classification very slow. Thirdly, the dataset is not diverse and does not include images captured in varying lighting effects and environmental conditions. Fourthly, integrating these models into a real-time inspection system is challenging because of processing speed and always needs more data than is feasible in the practice.

CHAPTER 4

Crack Detection in Solar Panel Using B-Net Deep Learning Model

4.1 Overview

In this proposed work we designed the new B-Net Model for identifying cracks in solar panel using deep learning techniques. This work aims to enhance the performance and the accurate detection of cracks in solar panels. The vital contribution of research is to develop a model that can find cracks in varying lighting and weather conditions. This research plays a role in a safe and clean environment and helps to reduce global warming. The architecture and methodology involving various stages are given below in the methodology section.

4.2 Problem Statement

The use of solar systems has increased rapidly worldwide due to the shortage of clean and renewable energy resources. The issue is to detect cracks in solar panels. We aim to address the challenge of identifying and locating cracks in solar panel surfaces. The problem of cracks badly reduces the performance of solar panels, leading to reduced energy production. The objective is to make a reliable and efficient crack detection system using convolutional neural network architecture particularly, deep learning models, to ensure the optimal functioning of solar panels and enhance their longevity.

The first objective is to check the ability of the proposed B-Net algorithm to detect cracks on PV modules under varying environmental conditions, including changes in lighting and weather, and evaluate how these conditions impact the algorithm's accuracy in crack detection. Secondly, to compare the accuracy and efficiency between the B-Net model and traditional methods for crack detection on PV modules, to determine the relative effectiveness and practicality of each approach in real-world applications.

4.3 Methodology

The section on methodology for the proposed work has several crucial steps. It starts with dataset preparation.

4.3.1 Dataset Preparation

We collect high-resolution images of PV panels. It ensures that these images are diverse, including both non-crack and cracked panels. To remove any low-quality and corrupted images, the cleaning process is implemented throughout the dataset. It ensures that only high-quality images are used in the training and validation process. Moreover, all images are standardized to a uniform resolution such as 224x224, 512x512, and 1024x1024, etc. We use consistent color space that is RGB (red, green, blue) for effective model training.

4.3.2 Data Collection and Annotation

This research represents a collection of datasets of solar panels (cracked and non-cracked) from Pakistan and additionally, from the Kaggle website then these datasets merged. In our data set, we take 3007 RGB images. It consists of 1431 images of non-crack or clear panels and 1571 images of crack panels. These images are passed through the annotation process by using efficient tools. The annotation process precisely labels the type, presence, and structural geometry of cracks. The dataset collection is shown in Table 4.1.

Dataset	**Number of Images**
Cracked	1576
Non-Cracked	1431
Total	3007

Table 4.1: Dataset Collection

4.3.3 Train/Validation/Test Set Split

To assess model performance, we established a well-defined train/validation/test set to split as subsets for the dataset. The dataset is divided into three subsets for example 60, 70, and 80 percent for training, 20, 15, and 10 percent for validation, and 20, 15, and 10 percent for tests respectively. This hierarchal approach ensured the representation of three classes of each subset. This approach enables the model to learn and understand effectively. It also allows neutral performance assessment. The training subset is used to train our B-Net model, the validation

subset is used to tune hyper-parameters and observe performance to mitigate overfitting, and the test subset is used for output or final evaluation. This output result shows the capability of the model to detect cracks for new unseen data. By employing this methodology, the proposed work objective is to develop a strong B-Net model that can correctly detect cracks in solar panels and contribute to the reliability and longevity of solar systems.

4.4 Proposed B-Net Model

B-Net Convolutional Neural Network architecture is designed to improve image processing tasks, specifically for crack detection in solar panels, aiming to optimize solar energy systems. We develop an innovative deep-learning model, to distinguish cracked and non-cracked solar panel images. It builds upon the fundamental principle of traditional CNNs and uses advanced techniques like batch normalization, and dropout layers. The model contains five convolutional layers, five pooling layers, and a dense layer. This layout aims to produce high output in crack extraction. It decreases the number of parameters and aims to keep low computational costs. B-Net architecture is characterized by its modules and depth, enabling it to understand complex patterns from huge datasets and maintain computational efficiency. This architecture consists of input layers, flattened, dense layers, and output layers. The architecture of B-Net is shown in Figure 4.1. (author own created figure)

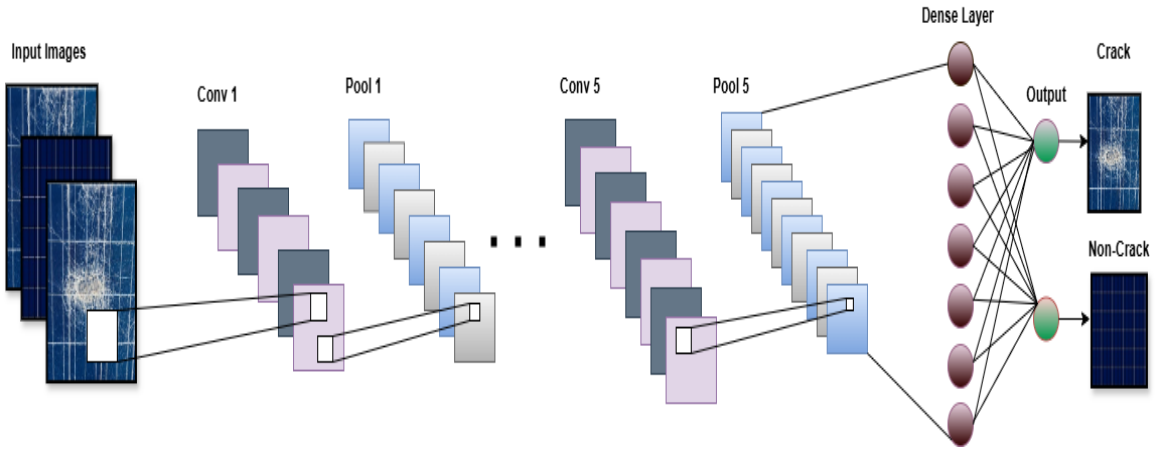

Figure 4.1: Architecture of B-Net (Proposed Model)

4.5 Training Environment, Tools, and Settings

This step describes the technical environment, tools, and settings deployed to train the model. It ensures the efficiency and reproducibility in B-Net model development. These are

carefully selected to enhance the model's training process. The model uses fine-tuning hyper-parameters, GPU acceleration, and essential libraries for efficient training, ensuring reliable performance and high accuracy on classification tasks. Python was used because of its extensive tools and libraries for ML and DL. Table 4.2 shows the tools used in training the proposed model. Table 4.2 shows the environment and tools used in the proposed work.

Environment and Tools	
Hardware	Intel Core i5 (GPU), 6th Generation
Operating System	Window 10
Programming Language	Python 3.12.3 (64-bit)
Deep Learning Framework	TensorFlow 2.15.0
Integrated Development Environment (IDE)	Google Colab

Table 4.2 Tools Used in Proposed Work

Table 4.3 shows settings, performance metrics, and splitting of the dataset used in the proposed model to make it efficient. Data augmentation was used to improve the performance of B-Net. Evaluation metrics such as accuracy, precision, recall, and F1-score ensured the effectiveness of the model.

Settings	**Values**
Data Augmentation Method	Applied
Total Dataset	3007 RGB Images
Splitting of Dataset	Training (80%) + Test (20%) Split
Evaluation Metrics	Accuracy, Precision, Recall, F1-Score

Table 4.3 Settings, Performance Metrics, Dataset Split

Hyper-Parameter tuning is a crucial step during training. In this procedure, we optimize the training parameters and architecture of the model to obtain the finest performance. Some hyper-parameters are learning rate, batch size, number of epochs, and dropouts. In the proposed B-Net model different values of these parameters are used while the best results are achieved, shown in Table 4.4.

Hyper-Parameter	**Values**
Learning Rate	0.0001
Batch Size	64
Loss Function	Binary Cross Entropy
Optimizer	Adam (Adaptive Moment Estimation)
Number of Epochs	100
Early Stopping	Applied
Activation Function	Sigmoid
Dropout Rate	0.025
Pooling Size	2 x 2
Number of Layers (convolutional + fully connected)	5+ 1 = 6

Table 4.4 Hyper-Parameters and Values

4.5.1 Work Flow of Proposed Work

The workflow of the proposed model is shown in Figure 4.2. The diagram represents the process of dataset preparation, training, and testing of the convolutional neural network B-Net model for crack detection on images of solar panels. The workflow illustrates the pipeline from data preparation to the final evaluation. The B-Net learns from labeled images of cracked and

non-crack solar panels in the training phase, and then the model's performance is validated using the testing dataset.

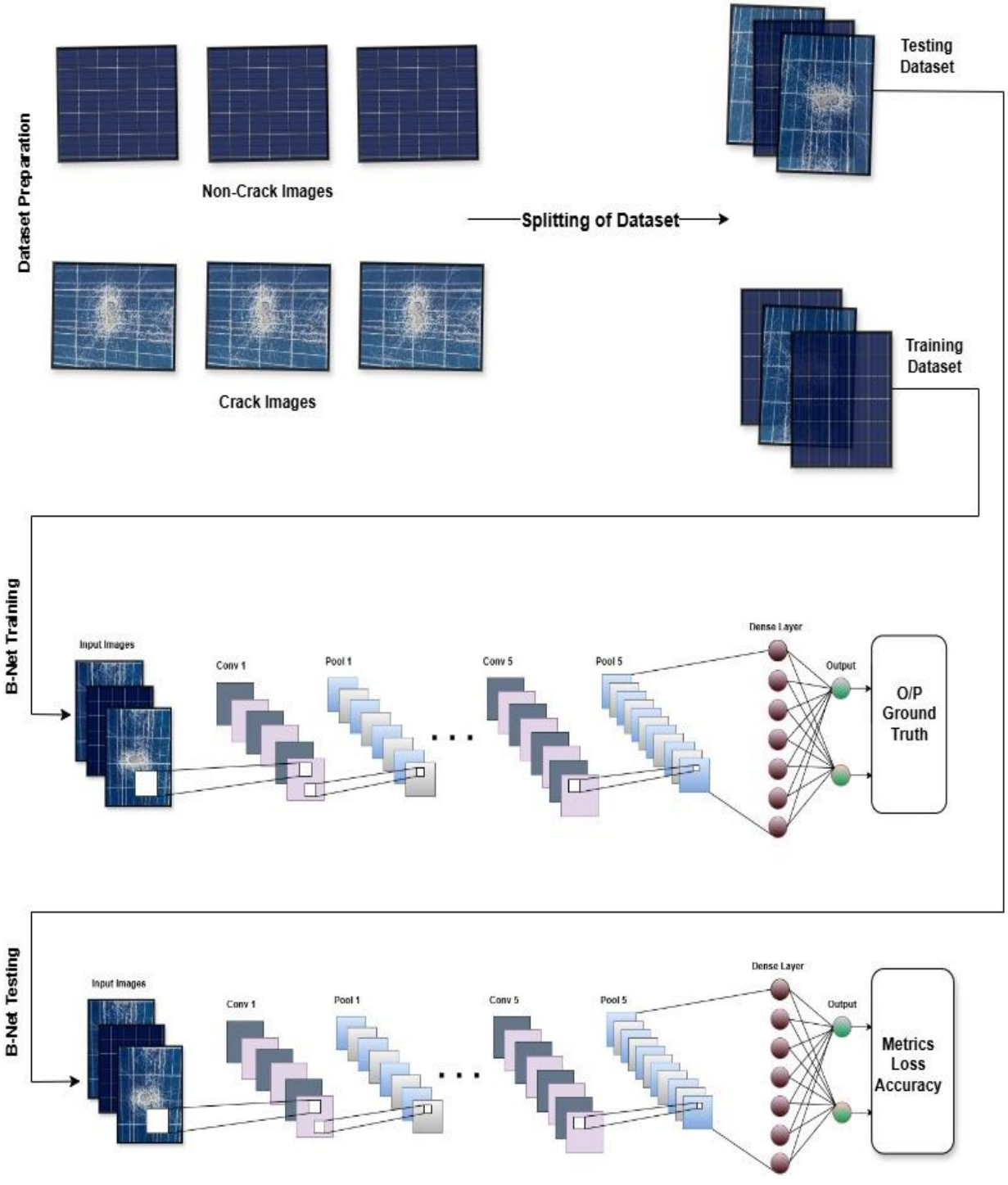

Figure 4.2: Work Flow of Proposed Work

4.5.2 Loss Function and Optimization Algorithm

The model's training starts with choosing the suitable loss function and optimization algorithm. These two are important for guiding the model's learning process. The loss function measures the difference between the actual labels and the predicted outputs. It provides feedback to the model in the training procedure. We use binary cross-entropy as a loss function because our dataset has two classes. Binary cross-entropy is one of the best options for binary classification tasks. Further, it is extended into categorical cross-entropy.

$$Binary\ Cross - Entropy = -[\mathbf{y} \cdot log(\hat{\boldsymbol{y}}) + (\mathbf{1} - \mathbf{y}) \cdot log(\mathbf{1} - \hat{\boldsymbol{y}})] \quad (8)$$

Where,

$\hat{y} \in (0,1)$ is the predicted probability of each class and $y = \{0,1\}$ is the true class label.

Optimization Algorithm:

Optimization algorithms are employed to minimize the loss function. In it, we adjust the model's weights. We use Adam (Adaptive Moment Estimation) as an optimization algorithm in the proposed B-Net model. We preferred it because of its adaptive learning rate capability. It is helpful to converge faster. It is efficient for training models because this algorithm composites the benefits of both momentum and root mean square propagation optimization algorithms. Adam works well for large and complex datasets. It has some cons, as it leads to overfitting in some cases when hyper-parameters do not tune well.

4.5.3 Early Stopping and Model Selection

Early stopping monitors the model's performance during training on the validation dataset and finishes the training when the model's performance degrades. It shows that the model does not generalize the dataset, but it memorizes the training data. We use the following parameter in this step, shown in Table 4.5.

Patience	Mode	Restore_best_weight	Monitor
10	Minimum	True	val_loss

Table 4.5 Early Stopping and Values

4.5.4 Data Augmentation Techniques

Data augmentation techniques are used to enhance the model's generalization capability. It also reduces overfitting during the training of the model. There are several data augmentation techniques. It includes real-time data augmentation applied using an image data generator in keras, rotation range up to 30 degrees, width and height shifts up to 30% of image size, shear transformation of range 0.3, zoom range by the factor of 0.3, and horizontal flip to mirrored images and fill mode used to handle blank area created due to transformation of images. It helps the model to understand and recognize cracks from various perspectives and angles. These are used to enhance the model and help it understand and learn more generalized features.

4.6 Results and Analysis

This section demonstrates the findings and insights from testing different models on the given dataset. The comparison of performance metrics, including accuracy, precision, recall, and F1-score, shows the effectiveness of each model. This analysis helps to understand the weaknesses and strengths of different models.

4.6.1 Pre-Trained Models

The following pre-trained models are commonly used and have good performance metrics. In this research, we trained these models on our dataset and observed accuracy, precision, recall, F1-score, and loss results.

1. MobiNet-V2

MobiNet-V2 provides moderate performance with an accuracy of approximately 52% in the classification task. The precision and recall are equal to 51.75%, showing a consistent level of performance. F1-score is 51.7470896244049%. However, the high loss of 7.5897 demonstrates that the model struggles to learn and understand from the given training dataset. This combination of high loss and moderate accuracy indicates that MobiNetV2 may not be reliably differentiated between the two classes. This shows the limits of overall effectiveness on datasets with images captured in diverse lighting and weather conditions.

2. ResNet50

It provides strong performance, achieving an accuracy of 80% in the classification task. It exhibits consistent balance throughout evaluation metrics, all achieving 80%, demonstrating that

the model effectively differentiated between positive and negative cases. Moreover, the ResNet50 model has a loss value of 0.4506, which is very low comparatively, indicating that the model effectively learned from the given dataset. ResNet50's solid performance metrics exhibit that it is a competitive option in several classification scenarios.

3. Inception_V3

Inception_V3 exhibits an accuracy of approximately 51%. This model also shows consistent behavior across evaluation metrics. It provides a high loss of 8.1797, indicating that it may struggle to learn from the training dataset. This combination of high loss and low accuracy demonstrates that overall effectiveness is limited across datasets that have images captured in diverse lighting and weather conditions.

4. VGG16

VGG16 model attains an accuracy of 47%, which shows that the model correctly learns and identifies only 47% from training data. The result is mirrored across the performance metrics, showing the consistency of the model. It has a loss of 0.8637, exhibiting that the model may not learn from given training data because low loss is correlated to high performance.

4.7 Experimental Results of B-Net Architecture

In this step, we analyze the impact of changing values of different hyper-parameters on the performance of the B-Net architecture.

ID	Image Size	Dense Layers	Dropouts	Accuracy (%)	Precision (%)	Recall (%)	F1-score (%)
1	128	512+1024	Nil	87.15	87.15278	87.15278	87.1527791023254
2	256	512+1024	Nil	91.67	91.66667	91.66667	91.6666686534881
3	512	512+1024	Nil	91.67	91.66667	91.66667	91.6666686534881
4	512	512+1024	0.025	94.44	94.44	94.44	94.4444417953491

Table 4.6 Results Based on Different Image Size

Table 4.6 provides the results of experiments conducted to assess the performance of the B-Net model under varying hyper-parameters, assigned a unique ID or Model No. We change image size while other components are set constant or unchanged, such as batch size of 64, epochs 32, convolutional layers 5, dense layers 2 (512+1024), and dropouts, while changing

image size provides specific accuracy, precision, recall, and F1-score. The training, validation, and test sets are 80%, 10%, and 10% same for further tables.

Analysis of the table or data shows that Model 1, with image size 128 (pixels), acquires an accuracy of 87.15%, Model 2 and Model 3 achieve identical accuracy of 91.67% with image sizes 256 and 512, and Model 4 provides superior accuracy of 94.44% utilizing image size 512. This indicates a correlation between model accuracy and image size. Moreover, adding a dropout layer of 0.025 rate in Model 4 significantly improves accuracy to prevent overfitting. Thus, the table is a helpful resource for comparing the efficiency of several B-Net architectures and hyper-parameters in a given task and explains the impact of various factors on model performance.

ID	Image Size	Dense Layers	Dropouts	Accuracy (%)	Precision (%)	Recall (%)	F1-score (%)
5	256	2048	0.025	89.93056	89.93056	89.93056	89.9305582046508
6	256	2048	0.0025	90.27778	90.27778	90.27778	90.2777791023254
7	256	2048	0.001	92.01389	92.01389	92.01389	92.0138895511627
8	256	2048	0.0001	94.09722	94.09722	94.09722	94.097226858139
9	256	2048	0.005	94.44444	94.44444	94.44444	94.4444417953491
10	512	2048	0.005	93.06	93.06	93.06	93.0555582046508

Table 4.7 Results Based on Different Dropouts

Table 4.7 provides the results of experiments conducted to assess the performance of the B-Net model under varying hyper-parameters. Each row includes key parameters such as image size, batch size, epochs, convolutional and dense layers, dropout rates, accuracy, precision, recall, and F1-score in percentage. In the above table, all tests except the last one utilize image size 256 (pixel), while the last one uses 512. A consistent 32 epochs, batch size 64, five convolutional layers, and 2048 dense units deployed for feature extraction were maintained throughout all experiments.

The results show that the dropout rate critically impacts the performance of the model. By decreasing the dropout rate from 0.025 to 0.0001, the accuracy significantly increases. It reveals that decreasing the dropout rate allows the model to effectively prevent the loss of important features. The greatest accuracy of 94.44% was attained with a 0.005 dropout rate (ID 9). Noticeably, the model utilized an image size of 512 pixels (ID 10) and achieved an accuracy

of 93.06%, a minor lower than small image size tests, which shows that larger images contain more detail and introduce complexity that impacts the learning efficiency.

ID	Image Size	Batch Size	Dropouts	Accuracy (%)	Precision (%)	Recall (%)	F1-score (%)
11	512	16	0.025	50.00	0	0	Nan
12	512	32	0.025	93.4	93.4	93.4	93.4027791023254
13	512	64	0.4	57.29167	57.29167	57.29167	57.2916686534881
14	256	64	0.1	92.36111	92.36111	92.36111	92.36111
15	512	64	0.05	93.40278	93.40278	93.40278	93.4027791023254
16	512	64	0.025	95.13889	95.13889	95.13889	95.1388895511627
17	512	64	0.015	90.625	90.625	90.625	90.625
18	512	64	0.005	90.27778	90.27778	90.27778	90.2777791023254
19	512	128	0.025	92.36	92.36	92.36	92.3611044883728

Table 4.8 Results Based on Different Batch Size and Dropouts

Table 4.8 provides the results of experiments conducted to assess the performance of the B-Net model under varying hyper-parameters. Each row includes key parameters such as image size, batch size, epochs, convolutional and dense layers, dropout rates, accuracy, precision, recall, and F1-score in percentage. In the above table, all tests utilize image size 512 (pixel), while the ID 14 uses 256. Batch sizes vary from 16, 32, 64, and 128. A consistent 32 epochs, five convolutional layers, and 1024 dense units deployed for feature extraction were maintained throughout all experiments.

Analysis shows significant volatility in model performance. Interestingly, ID 11 reveals poor performance, which is only 50% accuracy. This is because of a low batch size of 16 combined with a high dropout rate of 0.025, which minimizes effective learning. On the other hand, ID 12 provides high performance with an accuracy of 93.4%, which shows that a larger batch size of 32 can increase effective learning. ID 13 achieved a low accuracy of 57.29% with a higher dropout rate of 0.4 and poor recall and precision score, demonstrating that a higher dropout rate can lead to a negative impact on model performance. ID 16 achieved the best

performance with an accuracy of 95.14%, precision, recall, and F1-score attained around 95%, demonstrating that this configuration is highly effective for classification tasks. Further, ID 14 provides good results with an accuracy of about 92.36%, showing that strong performance can be attained even if a small image size is used with appropriately tuned hyper-parameters. Changes in batch size critically influence model performance, showing that increasing the batch size from 16 to 32 significantly enhances accuracy. For instance, larger batch sizes do not always achieve high results, batch size 128 (ID 19) attains approximately 92.36% accuracy, in contrast, batch size 64 (IDs 14 and 15) achieves high accuracies.

ID	Image Size	Batch Size	Dense Layers	Accuracy (%)	Precision (%)	Recall (%)	F1-score
20	256	64	1024	92.355	92.355	92.355	92.355
21	256	128	1024	93.40278	93.40278	93.40278	93.4027791023254
22	256	256	1024	90.27778	90.27778	90.27778	90.2777791023254
23	512	32	1024	90.97	90.97	90.97	90.97
24	512	64	1024	93.4	93.4	93.4	93.4

Table 4.9 Results Based on Different Image Size and Batch Size

In Table 4.9, the model is tested on two image sizes, 256 and 512 pixels, with batch sizes from 32 to 256. A consistent 32 epochs, five convolutional layers, and 1024 dense units deployed for feature extraction were maintained throughout all experiments. No dropouts were used to simplify the architecture. Also, the risk of overfitting is increased. The model's accuracy, precision, recall, and F1-score varied between 90.28% to 93.40%. ID 21 achieved higher accuracy with batch size 128 and image size 256. ID 22 provides lower accuracy with batch size 256 and image size 256. This shows that smaller batch size improves model performance after potential tuning.

ID	Convolutional Layers	Dense Layers	Dropouts	Accuracy (%)	Precision (%)	Recall (%)	F1-score
25	4	2048	0.00001	91.31944	91.31944	91.3194	91.319441795
26	3	2048	0.00001	92.01389	92.01389	92.0138	92.013889551
27	3	1024	0.00001	92.01389	92.01389	92.0138	92.013889551
28	3	512 + 1024	0.00001	93.40278	93.40278	93.4027	93.4027791023

Table 4.10 Results Based on Different Convolutional and Dense Layers

All tests are processed with a consistent 256 image size, 32 epochs, and 64 batch size. Convolutional layers varied from 3 to 4 for feature extraction. The dense units differ, such as 1024, 2048, and 512+1024. We employed a low dropout rate of 0.00001 across the model to prevent overfitting and maintain learning flexibility. The model's accuracy, precision, recall, and F1-score varied between 91.32% to 93.40%. ID 28 achieved higher accuracy with a combination of dense units 512+1024 and three convolutional layers. This demonstrates that variations in dense units and some convolutional layers significantly impact model performance. Table 4.10 shows a suitable combination of dense layers can improve the model performance.

ID	Train+ Test	Epochs	Dense Layers	Accuracy (%)	Precision (%)	Recall (%)	F1-score (%)
29	80+20	32	512+1024	94.44444	94.44444	94.44444	94.4444417953491
30	80+20	32	512+1024	88.88889	88.88889	88.88889	88.8888895511627
31	80+20	32	512+1024	93.40278	93.40278	93.40278	93.4027791023254
32	80+20	32	256+512 +1024	90.27778	90.27778	90.27778	90.2777791023254
33	80+20	32	2048	90.97222	90.97222	90.97222	90.9722208976745
34	80+20	32	1024	90.625	90.625	90.625	90.625
35	80+20	32	1024	98.26389	98.26389	98.26389	98.2638895511627
36	80+20	70	1024	92.01389	92.01389	92.01389	92.0138895511627
37	80+20	100	1024	94.09722	94.09722	94.09722	94.097226858139
38	80+20	500	1024	94.79167	94.79167	94.79167	94.7916686534881
39	70+20 +10	32	1024	86.11111	86.11111	86.11111	86.1111104488372
40	60+40	32	1024	90.27778	90.27778	90.27778	90.2777791023254
41	70+10 +20	32	1024	91.31944	91.31944	91.31944	91.3194417953491

Table 4.11 Results Based on Different Dense Layer and Data Splits

All models tested on image size 512 except IDs 29 and 30, which use 256, consistent convolutional layers five except IDs 29 and 30, which use three, and consistent dataset split 10% test sample, 10% validation sample, and 80% training sample. Epochs vary from 32 to 500, improving learning and maximizing the risk of overfitting. The dense layers vary in the model, such as 1024, 2048, 512+1024, and 256+512+1024. Dropout varies from 0.00001 to 0.025; IDs 29 and 30 utilize 0.00001, and the rest use 0.025, preventing overfitting and under fitting while

excessively high can reduce learning. All tests were processed on a batch size of 64, as shown in Table 4.11.

The model's accuracy, precision, recall, and F1-score varied between 86.11% to 98.26%. ID 35 achieved higher accuracy with a single dense layer of 1024, an image size of 512, and 5 convolutional layers, while ID 36 provided lower accuracy. It demonstrated that deep networks often provide better accuracy, and other hyper-parameters also play a significant role in evaluating model effectiveness. All tests/experiments and analyses show valuable information for practitioners who want to optimize their convolutional neural network architectures by tuning hyper-parameters and balancing complexity.

ID	Image Size	Dense Layers	Dropouts	Accuracy (%)	Precision (%)	Recall (%)	F1-score (%)
4	512	512+1024	0.025	94.44	94.44	94.44	94.4444417953491
8	256	2048	0.0001	94.09722	94.09722	94.09722	94.097226858139
9	256	2048	0.005	94.44444	94.44444	94.44444	94.4444417953491
16	512	1024	0.025	95.13889	95.13889	95.13889	95.1388895511627
28	256	512+1024	0.00001	93.40278	93.40278	93.40278	93.4027791023254
29	256	512+1024	0.00001	94.44444	94.44444	94.44444	94.4444417953491
35	512	1024	0.025	98.26389	98.26389	98.26389	98.2638895511627
37	512	1024	0.025	94.09722	94.09722	94.09722	94.097226858139
38	512	1024	0.025	94.79167	94.79167	94.79167	94.7916686534881

Table 4.12 Important Results

These are important results of the B-Net model during tuning hyper-parameters shown in Table 4.12. The accuracy of the model varies from 93.40% to 98.26%. During changes, it provides approximately 94%; after proper and suitable tuning, it gives more than 98% accuracy. The highest accuracy was achieved with an image size of 512 pixels, a dense layer of 1024, a dropout rate of 0.025, and five convolutional layers with 16, 64, 8, 16, and 64 filters. This analysis demonstrates that a suitable image size and dense layer can significantly improve performance.

4.8 Performance Metrics of B-Net Model

Among the above results, the highest performance is mentioned in Table 4.13, which shows that accuracy can be enhanced with proper hypermeter tuning and annotation techniques.

Accuracy	Precision	Recall	F1-score
98.26%	98.264%	98.26%	98.263889%

Table 4.13 Performance Metrics of B-Net Model

4.8.1 Accuracy

$$Accuracy = \frac{TP+TN}{TP+FP+TN+FN} \quad \text{Eq. (1)}$$

The line chart in Figure 4.3 represents the proposed model's training and validation accuracy over the different epochs. The x-axis depicts the epochs, which are iterations of training the B-Net on the dataset. The y-axis shows the model's accuracy. The range of accuracy is from 0 to 1. The value 1 illustrates perfect accuracy. The blue line represents the accuracy of the training dataset, and the orange line represents the accuracy of the validation dataset.

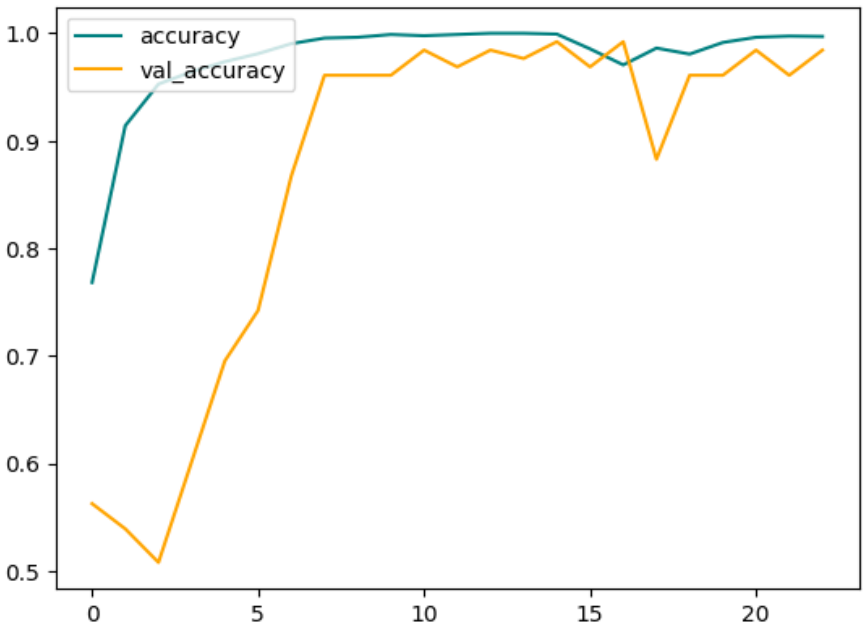

Figure 4.3: Accuracy of B-Net

4.8.2 Precision

$$Precision = \frac{True\ Positives}{True\ Positives + False\ Positives} \quad \text{Eq. (2)}$$

Figure 4.4 illustrates the proposed model's training and validation precision over the different epochs. The x-axis represents the epochs, which are iterations of training the B-Net on the dataset. The y-axis presents the model's precision. The range of precision is from 0 to 1. The value 1 shows perfect precision. The blue line illustrates the precision of the training dataset, and the orange line illustrates the precision of the validation dataset.

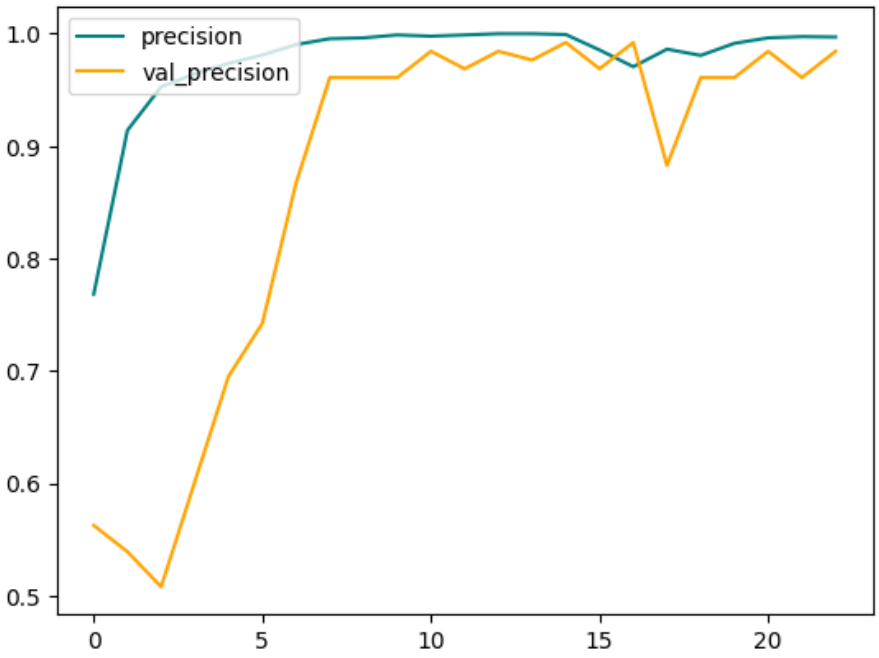

Figure 4.4: Precision of B-Net

4.8.3 Recall

$$Recall = \frac{True\ Positives}{True\ Positives + False\ Negatives} \quad \text{Eq. (3)}$$

The line chart shows the proposed model's training and validation recall. The x-axis represents the epochs, which are iterations of training the model on the dataset. The y-axis represents the model's recall. The blue line shows the recall of the training dataset, and the orange line shows the recall of the validation dataset. Shown in Figure 4.5.

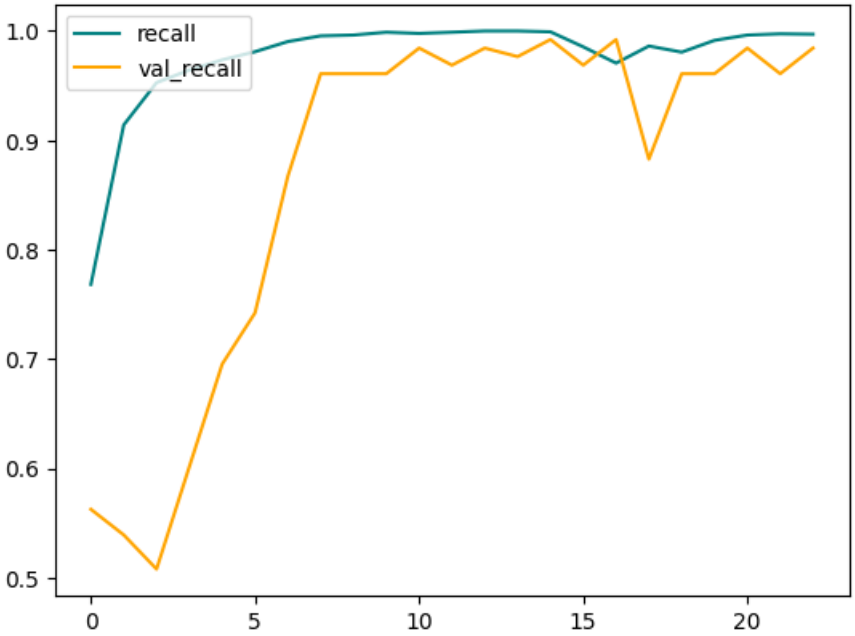

Figure 4.5: Recall of B-Net

4.8.4 Loss

Figure 4.6 indicates the proposed model's training and validation loss across several epochs. The x-axis illustrates the epochs and the y-axis illustrates the loss value of the proposed model, ranging from 0 to 1. The value 1 shows low performance and 0 shows perfect performance. The blue line represents the loss of the training dataset, and the orange line represents the loss of the validation dataset.

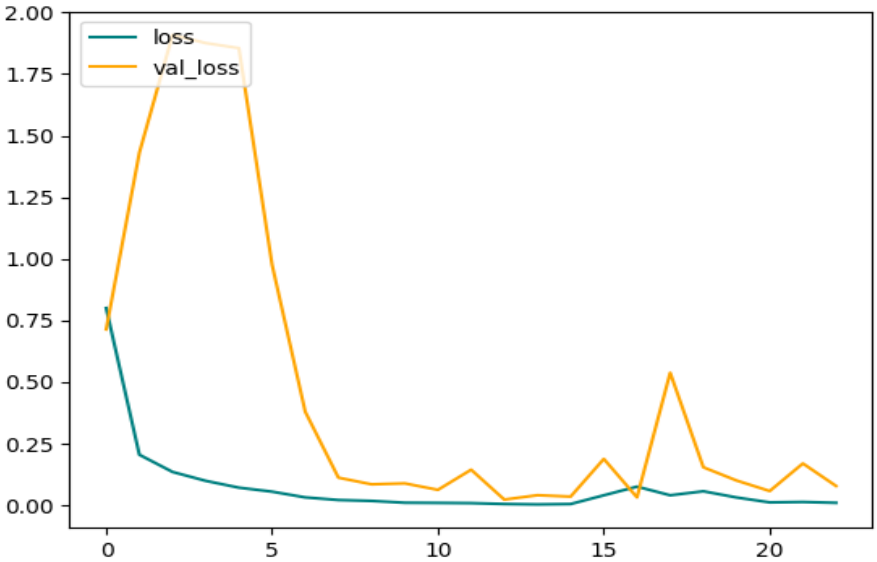

Figure 4.6: Loss of B-Net

4.9 Confusion Matrix

The confusion matrix of the proposed B-Net model for crack detection shows how well the model differentiates between ‘Non-Crack’ and ‘Crack’ panels. Figure 4.7 shows the results for each element of this matrix.

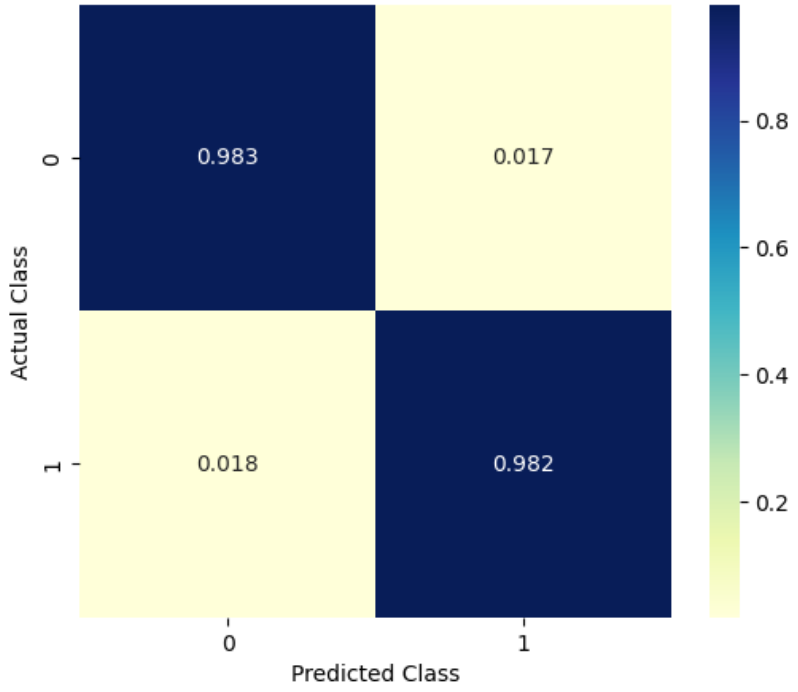

Figure 4.7: Confusion Matrix for Crack Detection

True Negative: The value of the top left element of the matrix is 0.983. The B-Net correctly predicts ‘Non-Crack’ when a crack is absent on the panel. The prediction occurred 98.3% of the time.

False Positive: The value of the top right element is 0.017 showing the B-Net predicted ‘Crack’ when there wasn’t a crack on the panel. This happened 1.7% of the time.

False Negative: The bottom left element is 0.018. The B-Net predicted ‘Non-Crack’ when the panel had a crack. This occurred 1.8% of the time.

True Positive: The bottom right element is 0.982. The B-Net correctly predicted ‘Crack’ when the panel had a crack. This happened 98.2% of the time. The proposed model exhibits high accuracy and low misclassification rate in both directions.

4.10 Comparison Across Training and Testing Dataset

Here the proposed model is examined during the training and testing dataset which shows how well the model is performed during training and testing. The results in Table 4.14 show that B-Net trained very well on a given dataset.

Model	Dataset	Accuracy	Precision	Recall	F1-Score
B-Net	Training	0.9934157	0.9934157	0.9934157	0.993415725
	Testing	0.9826389	0.9826389	0.9826389	0.9826388955
	Difference	0.0107768	0.0107768	0.0107768	0.0107768295

Table 4.14 Performance of B-Net across Training and Testing Dataset

Figure 4.8 shows that B-Net is trained very well on a given dataset as compared to a testing dataset with slight differences between them. The low difference shows that proposed predictions are outperforming.

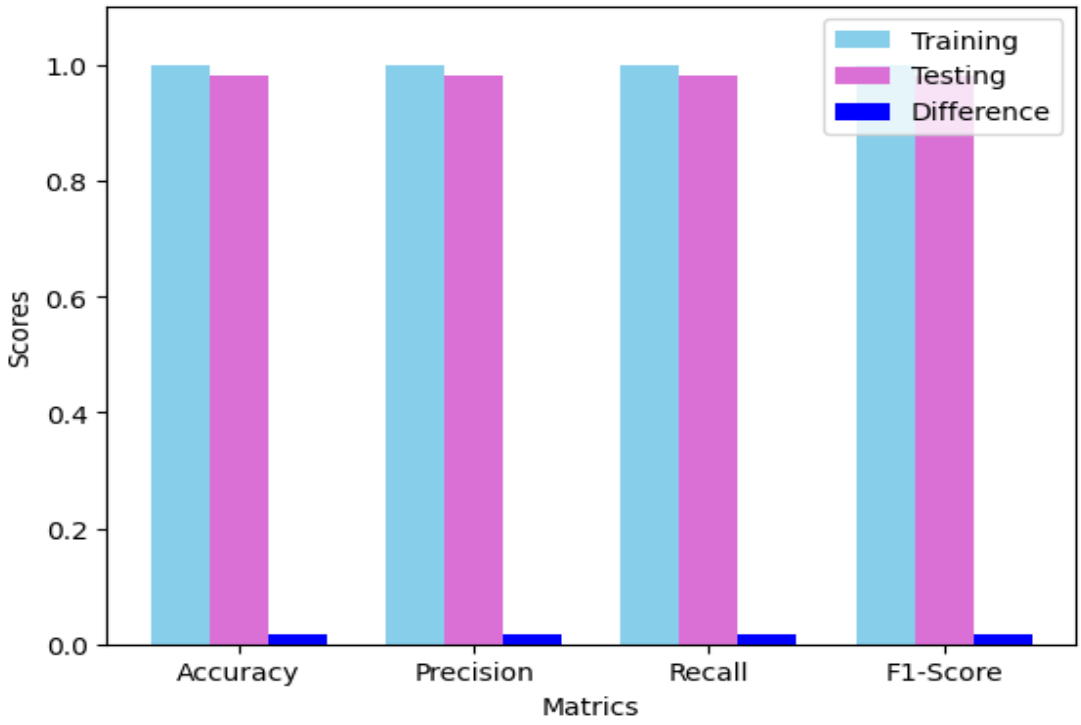

Figure 4.8: Performance of B-Net on Training and Testing Dataset

4.11 Comparison to Other Models

Table 4.15 compares the performance of the B-Net model to other CNN models, showing the proposed model performs better.

Models	Accuracy	Precision	Recall	F1-score	Loss
MobiNet-V2	0.5174709	0.5174709	0.5174709	0.517470896244049	7.5897
ResNet	0.8	0.8	0.8	0.800000071525573	0.4506
Inception_V3	0.50748754	0.50748754	0.50748754	0.507487535476684	8.1797
VGG16	0.47254574	0.47254574	0.47254574	0.472545742988586	0.8637
Proposed B-Net	0.9826389	0.9826389	0.9826389	0.982638895511627	0.0374

Table 4.15: Comparison to Other Models

4.11.1 Comparison of Accuracies

The bar chart compares the accuracy models for the given dataset. The compared models are MobiNet_v2, ResNet, Inception_v3, VGG16, and the proposed B-Net. VGG16 shows the lowest accuracy, and B-Net attained the highest accuracy. This demonstrates that the proposed model outperforms the other models on the given dataset shown in Figure 4.7.

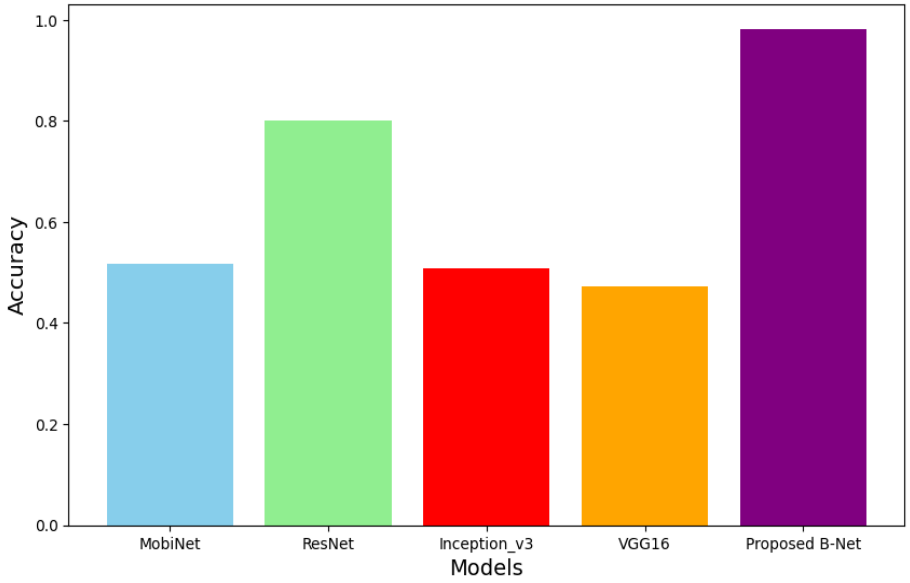

Figure 4.9: Accuracy Comparison

4.11.2 Comparison of F1-Scores

The bar chart compares different models' F1 scores. In this analysis, MobiNet_v2 has a moderate score, ResNet has a higher score, Inception_v3 is slightly lower than ResNet, VGG16 has a low F1 Score, and the B-Net outperforms all the other models shown in Figure 4.10.

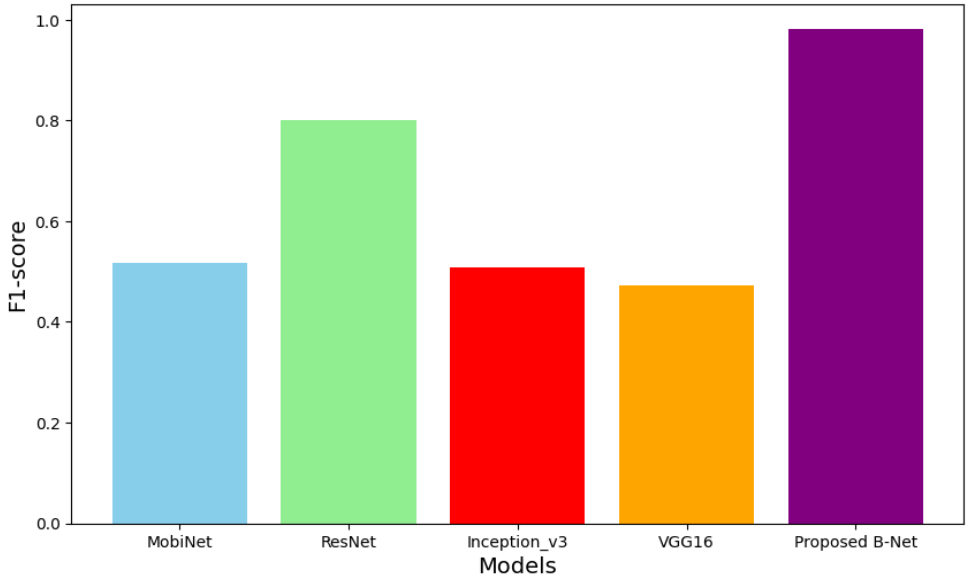

Figure 4.10: F1-Score Comparison

4.11.3 Comparison of Precisions

Figure 4.11 compares the precision of models. This comparison shows that the B-Net model outperformed the other models, exhibiting that it correctly identifies positive cases.

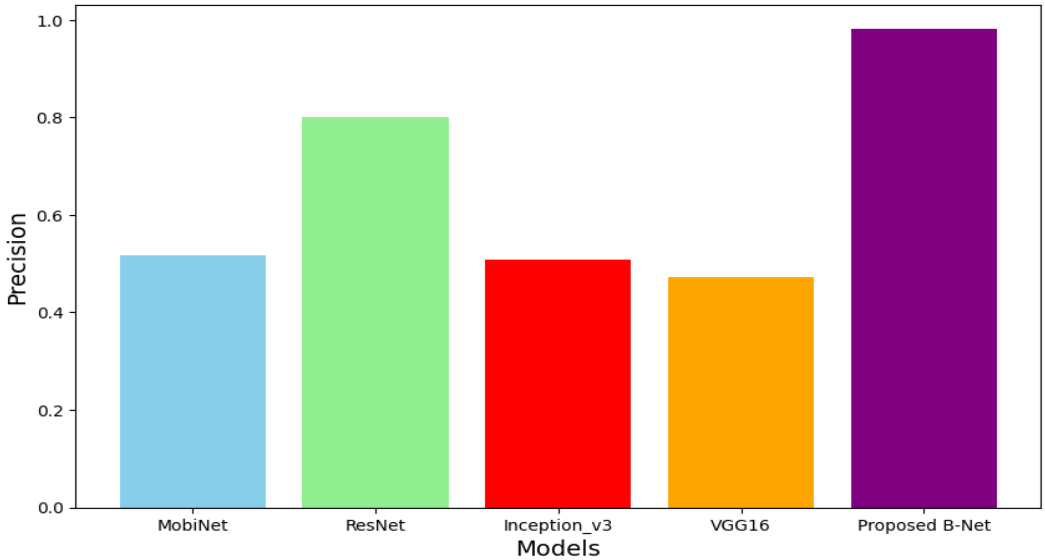

Figure 4.11: Precision Comparison

4.11.4 Comparison of Recalls

Figure 4.12 explains a recall comparison of models. In this analysis, VGG16 has a lower recall, and the proposed model outperforms all the other models, suggesting that it correctly predicted positive instances.

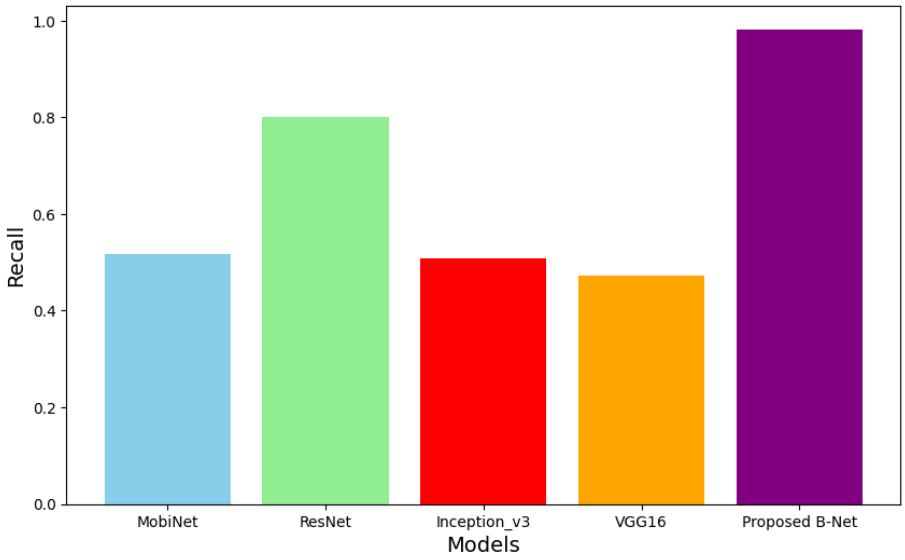

Figure 4.12: Recall Comparison

4.11.5 Comparison of Loss

Figure 4.13 compares the loss values of the models and shows that Inception_v3 is performing lowest and the B-Net outperformed other models. The high loss shows the low performance of the model.

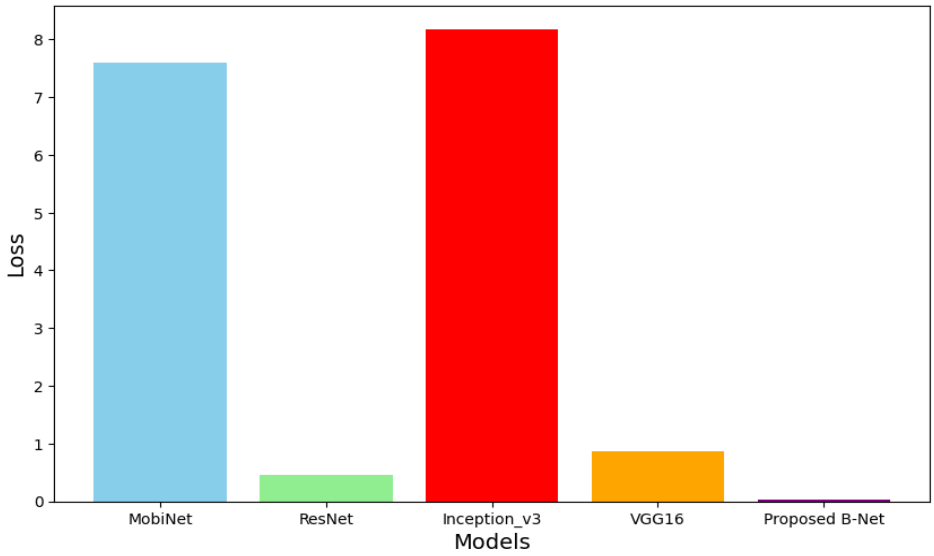

Figure 4.13: Loss Comparison

4.11.6 Comparison of Computational Cost

In this step, the proposed model is compared with other CNN models for computation cost, which illustrates the B-Net model trained a lower number of parameters than other models with the same dataset shown in Table 4.16.

Model	Number of Parameters (millions)
ResNet	21.3
Inception_V3	22.07
VGG16	17.93
MobiNet-V2	2.42
B-Net	12.8

Table 4.16 Comparison of Computational Cost

CHAPTER 5

CONCLUSIONS & FUTURE WORK

5.1 Conclusions

In our research, we have exhibited the capacity of the B-Net deep learning model for impressive crack detection in solar panels. Proper training and evaluation provide promising results in effectively identifying defects that could slow down the output of SE systems. This section summarizes the important findings from the study. We highlight the potential of the proposed architecture compared to traditional methods.

The B-Net model was trained and assessed on a diverse dataset of PV panel images containing different conditions and types of panels. The results show that B-Net reached an overall accuracy of 98.26% on the test set, with recall and precision metrics indicating the model's ability to detect cracks accurately. Moreover, the F1-score further evaluates the B-Net performance in finding defects within the images. The qualitative assessment indicated that the model effectively extracted both large and small cracks encompassing different orientations. It shows the model's adaptability and robustness. The effectiveness of the B-Net was emphasized by its capability to generalize encompassing different types of panels, lighting effects, and varying environmental conditions. It achieved high extraction rates even under varying and challenging circumstances, like different weather conditions and illumination. Additionally, the integration of state-of-the-art architectural features, including data augmentation techniques, provides impressive performance. The qualitative analysis shows that the model not only finds visible cracks but also spotlights the areas where cracks could exist. It gives valuable awareness to maintenance teams. The traditional methods depend on simple algorithms and human expertise that would fail to observe narrow cracks and be affected by environmental factors. On the other hand, the B-Net model permits for automated inspections. It can proceed with large sizes of images faster while cutting back on human errors. The comparison illustrates that the proposed model outperformed these traditional methods in speed and detection accuracy. It

makes the model a more reliable solution for real-world automated monitoring systems for solar panels. This research demonstrates that significant enhancements were made possible by using CNN deep learning technologies such as the B-Net model.

The key contributions to the field are the focus on the novelty of the approach and the impact of this research on the maintenance and monitoring of solar panels. These contributions illustrate the practical value and highlight the advancement in SE technologies enabled by this research. The B-Net model presents a novel approach that uses modern CNN architectures developed for image analysis. B-Net employs deep learning for automated inspection systems and accurately identifies cracks. The techniques used in B-Net architecture such as data augmentation make the model adaptable to several critical circumstances. This innovative approach makes an efficient and smooth monitoring process and minimizes the dependency on human experts. So it reduces errors related to manual assessments.

The execution of the B-Net has an important role in PV panel inspection and maintenance practices. The model provides an automated solution for crack identification and enables a proactive approach to early detection for maintenance strategies. It prevents costly repairs and saves from critical damages. Regular inspection facilitated by the proposed model can boost energy output. It ensured that solar panels operate at maximum production. The undetected cracks decrease performance and magnify energy losses. Additionally, the capability to integrate B-Net into current monitoring systems improves operational effectiveness, enabling immediate judgment of panel health, and accommodating decision-making concerning maintenance. In this work, the research conducted opens the door for the comprehensive field of deep learning applications in crack extraction in various industries. By showing the efficiency of CNNs such as B-Net in detecting defects in panels, this research concretes the way for parallel methodologies to be employed in other contexts, like infrastructural monitoring, environmental inspections, and manufacturing quality control. The findings highlight the flexibility of deep learning techniques in automated crack detection processes. It can enhance efficiency and accuracy in contrast to conventional methods. This advancement improves operational efficiency across specific fields and encourages embracing AI-driven solutions in sectors where early crack identification is crucial for performance and safety.

5.2 Limitations

This section outlines the limitations of the work, focusing on challenges in data collection and model training, and problems related to robustness and generalization. It also suggests areas for future improvements. This research has made significant steps in developing the proposed model, but various constraints or limitations were encountered during the research process. One of the primary limitations was the accessibility of high-resolution labeled images or datasets for testing and training the B-Net model. The images or dataset employed in this study may not completely present the diversity of photovoltaic panel conditions such as types of panels, diverse defect types, and environmental factor influences. Moreover, time constraints bound the process of experimentation on several architectures and tuning of hyper-parameters that could optimize performance.

There are a lot of challenges during data collection in this research. Achieving a comprehensive dataset that has a large variety of crack types and conditions needed broad efforts in sourcing images from various installations and ensuring correct labeling by professionals. We collect images from sites including NUML, Pvt Ltd corporations, and residential areas. It is a tough task due to security policies, safety concerns, and documentation or permission letter requirements. We captured images in varying lighting like morning, noon, and evening, and different environmental conditions like sunny, cloudy, and rainy days which is time-consuming and needs more resources making it a difficult task. Additionally, the B-Net training process faced challenges due to diverse data which unstable the loss rate of the model. It is also a plus point that data is diverse and can provide good performance on test datasets. Another challenge is overfitting, especially due to the limited number of images in varying conditions. The data augmentation techniques improve the training set but there remains a risk that the model may not be robust and generalize properly on other images that are not a part of the training distribution.

The generalization ability of the proposed model is internally limited due to the dataset on which it was trained. On the other hand, B-Net provides good results and performs well on the test set. The model efficiency may vary when employed to various solar panel types or changing environmental factors that were not part of the training data. Furthermore, unusual lighting scenarios and extreme weather conditions may badly affect extraction accuracy, increasing the number of false positives or false negatives.

5.3 Future Work

Future research in this field of defect identification using CNN, particularly deep learning should devote effort to increasing the size of the dataset or using more images that include a more diverse range of crack characteristics, panel types, and environmental conditions. This can be achieved through the cooperation of solar energy providers to collect real-world data from several installations, improving the model's capability to generalize throughout various scenarios. Furthermore, collaborating momentary data, like images taken over time, could provide a clear and immediate understanding of defect progression and enable predictive maintenance schemes. Further research can also find out the integration of sensor data such as humidity, temperature, light intensity, etc. with image analysis to enhance extraction accuracy and detailed understanding of cracks.

There are various avenues for enhancing the B-Net itself. One potential improvement is executing ultra-modern techniques such as transfer learning, which we use in this research. In transfer learning, pre-trained models are used after being fine-tuned for particular tasks like defect detection. So, B-Net can also be reused for another task after potential improvement. Moreover, deploying ensemble methods that unite multiple models, to achieve better results by employing a broader range of numerous features and minimize the rate of misclassifications. While using several models in the ensemble method trainable parameters and computational cost increase. Hyper-parameter optimization using automated techniques such as Bayesian optimization could be used to improve model efficiency.

The proposed model has provided promising results while using other deep-learning architectures may show valuable results in their efficiency for defect identification tasks. Models like MobiNet-v3, VGG16, VGG19, ResNet, Inception-v2, AlexNet, Improved AlexNet, and Improved ResNet, etc. could provide dominance in terms of computational efficiency and accuracy. Comparing B-Net and other architectures could help to determine weaknesses and strengths and be helpful for future model development customized especially for crack identification in solar panels.

The B-Net model introduced in this research can be extended beyond defect extraction in solar panels to find other types of cracks in different renewable energy technologies. This

approach could be employed to find faults in battery systems in SE storage solutions, wind turbine blades, and structural problems in hydropower installations. By expanding the scope of this study to add various types of faults throughout renewable energy technologies, the ability to enhance operational efficiency and maintenance practices can be effectively improved. It is also helpful to the overall sustainability of renewable energy systems.

5.4 Final Thoughts

Ongoing research in solar panel maintenance is crucial as the demand for and use of renewable energy continues to grow or extend globally. SE is a key player in the direction of sustainable energy systems. It also realized that the efficiency and longevity of solar panels is most important. This work effort focuses on modern inspection techniques, like deploying CNN models such as B-Net that can improve the capability to address and extract defects early. This proactive technique reduces maintenance costs and downtime and boosts energy output. It also plays a vital role in reliable energy supply. Progress in this field will be necessary to achieve the growing energy requirements and demands. It minimized the environmental impact due to conventional energy sources.

AI performs transformative contributions or functions in sustainable energy solutions. AI enhances several processes throughout the energy sector. Recent research highlighted that AI technologies can upgrade renewable energy predictions, enhance grid management, and allow timely maintenance of energy systems. By observing huge amounts of data from operational systems and sensors, AI can extract patterns that brief better decision-making. This ability strengthens operational effectiveness and assists the integration of renewable sources into present terminals and grids. It makes them more durable, flexible, and versatile to fluctuations in demand and supply. The alliance between renewable energy and AI is essential for enhancement in the direction of a sustainable future.

The future of solar energy systems and inspection methods is suspended for impressive advancements through progress in ML and AI. As renewable energy use spreads rapidly, we can look for smarter solar panels integrated with self-diagnostic ability that use AI algorithms to forecast and estimate maintenance needs and enhance performance depending on real-time data.

Moreover, combining AI with IoT (internet of things) such as gadgets, sensors, appliances, and other machines that share and gather across the Internet, will facilitate uninterrupted communication among monitoring systems and solar panels, enabling automated adjustments to magnify efficiency under varying conditions. This vision incorporates advancement in crack detection and enhanced overall management of PV energy systems, speeding up the adoption of solar systems worldwide, and contributing to a sustainable energy perspective.

References

[1] C. Kroeze, "Nitrous oxide and global warming," *Science of the Total Environment*, vol. 143, no. 2-3, pp. 193-209, 1994.

[2] Q. Li, W. Sun, B. Huang, W. Dong, X. Wang, P. Zhai, and P. Jones, "Consistency of global warming trends strengthened since the 1880s," 2020.

[3] P. V. Belolipetsky and S. I. Bartsev, "Hypothesis about mechanics of global warming from 1900 till now," Citeseer, 1900.

[4] S. K. Ritter, "Global warming and climate change," *Chem. Eng. News*, vol. 12, no. 21, pp. 11-21, 2009.

[5] M. L. Khandekar, T. S. Murty, and P. Chittibabu, "The global warming debate: A review of the state of science," *Pure and Applied Geophysics*, vol. 162, pp. 1557-1586, 2005.

[6] M. T. McCulloch, A. Winter, C. E. Sherman, and J. A. Trotter, "300 years of sclerosponge thermometry shows global warming has exceeded 1.5°C," *Nature Climate Change*, vol. 14, no. 2, pp. 171-177, 2024.

[7] S. Bernow, K. Cory, W. Dougherty, M. Duckworth, S. Kartha, M. Ruth, and M. Goldberg, "America's global warming solutions," *A study for the World Wildlife Fund and Energy Foundation*, Boston, MA: Tellus Institute, 1999.

[8] K. Williamson, A. Satre-Meloy, K. Velasco, and K. Green, "Climate change needs behavior change: Making the case for behavioral solutions to reduce global warming," *Rare: Arlington, VA, USA*, 2018.

[9] X. Zhang and I. Dincer, *Energy Solutions to Combat Global Warming*. Springer, 2017.

[10] D. S. Matawal and D. J. Maton, "Climate change and global warming: signs, impact and solutions," *International Journal of Environmental Science and Development*, vol. 4, no. 1, p. 62, 2013.

[11] M. Z. Jacobson, A.-K. von Krauland, S. J. Coughlin, E. Dukas, A. J. H. Nelson, F. C. Palmer, and K. R. Rasmussen, "Low-cost solutions to global warming, air pollution, and energy insecurity for 145 countries," *Energy & Environmental Science*, vol. 15, no. 8, pp. 3343-3359, 2022.

[12] D. Mitlin, "Sustainable development: A guide to the literature," *Environment and Urbanization*, vol. 4, no. 1, pp. 111-124, 1992.

[13] T. M. Parris and R. W. Kates, "Characterizing and measuring sustainable development," *Annual Review of Environment and Resources*, vol. 28, no. 1, pp. 559-586, 2003.

[14] I. Gunnarsdóttir, B. Davídsdóttir, E. Worrell, and S. Sigurgeirsdóttir, "Sustainable energy development: History of the concept and emerging themes," *Renewable and Sustainable Energy Reviews*, vol. 141, p. 110770, 2021.

[15] M. Jefferson, "Sustainable energy development: performance and prospects," *Renewable Energy*, vol. 31, no. 5, pp. 571-582, 2006.

[16] B. Nastasi, N. Markovska, T. Pukšec, N. Duić, and A. Foley, "Renewable and sustainable energy challenges to face for the achievement of Sustainable Development Goals," *Renewable and Sustainable Energy Reviews*, vol. 157, p. 112071, 2022.

[17] P. A. Østergaard, N. Duić, Y. Noorollahi, H. Mikulčić, and S. Kalogirou, "Sustainable development using renewable energy technology," *Renewable Energy*, vol. 146, pp. 2430-2437, 2020.

[18] Biomass Energy, "Renewable energy sources," *Ergon Energy*, 2015.

[19] P. Moriarty and D. Honnery, "What is the global potential for renewable energy?" *Renewable and Sustainable Energy Reviews*, vol. 16, no. 1, pp. 244-252, 2012.

[20] I. Dincer, "Renewable energy and sustainable development: a crucial review," *Renewable and Sustainable Energy Reviews*, vol. 4, no. 2, pp. 157-175, 2000.

[21] N. L. Panwar, S. C. Kaushik, and S. Kothari, "Role of renewable energy sources in environmental protection: A review," *Renewable and Sustainable Energy Reviews*, vol. 15, no. 3, pp. 1513-1524, 2011.

[22] S. R. Bull, "Renewable energy today and tomorrow," *Proceedings of the IEEE*, vol. 89, no. 8, pp. 1216-1226, 2001.

[23] G. Walker, "Renewable energy and the public," *Land Use Policy*, vol. 12, no. 1, pp. 49-59, 1995.

[24] A. Harjanne and J. M. Korhonen, "Abandoning the concept of renewable energy," *Energy Policy*, vol. 127, pp. 330-340, 2019.

[25] S. Carley, "State renewable energy electricity policies: An empirical evaluation of effectiveness," *Energy Policy*, vol. 37, no. 8, pp. 3071-3081, 2009.

[26] J. Zhong, M. Bollen, and S. Rönnberg, "Towards a 100% renewable energy electricity generation system in Sweden," *Renewable Energy*, vol. 171, pp. 812-824, 2021.

[27] A. Bahadori and C. Nwaoha, "A review on solar energy utilization in Australia," *Renewable and Sustainable Energy Reviews*, vol. 18, pp. 1-5, 2013.

[28] N. Kannan and D. Vakeesan, "Solar energy for future world: A review," *Renewable and Sustainable Energy Reviews*, vol. 62, pp. 1092-1105, 2016.

[29] F. M. Guangul and G. T. Chala, "Solar energy as a renewable energy source: SWOT analysis," *2019 4th MEC International Conference on Big Data and Smart City (ICBDSC)*, 2019, pp. 1-5.

[30] M. B. Hayat, D. Ali, K. C. Monyake, L. Alagha, and N. Ahmed, "Solar energy—A look into power generation, challenges, and a solar-powered future," *Int. J. Energy Res.*, vol. 43, no. 3, pp. 1049-1067, 2019.

[31] M. Bdour, Z. Dalala, M. Al-Addous, A. Radaideh, and A. Al-Sadi, "A comprehensive evaluation on types of microcracks and possible effects on power degradation in photovoltaic solar panels," *Sustainability*, vol. 12, no. 16, p. 6416, 2020.

[32] L. Bourgeois and E. Lunéville, "On the use of sampling methods to identify cracks in acoustic waveguides," *Inverse Problems*, vol. 28, no. 10, pp. 105011, 2012.

[33] K. Mazanoglu, "A novel methodology using simplified approaches for identification of cracks in beams," *Latin American Journal of Solids and Structures*, vol. 12, no. 13, pp. 2460-2479, 2015.

[34] G. L. Golewski, "The phenomenon of cracking in cement concretes and reinforced concrete structures: the mechanism of cracks formation, causes of their initiation, types and places of occurrence, and methods of detection—a review," *Buildings*, vol. 13, no. 3, p. 765, 2023.

[35] L. Li, Q. Wang, G. Zhang, L. Shi, J. Dong, and P. Jia, "A method of detecting the cracks of concrete undergo high-temperature," *Construction and Building Materials*, vol. 162, pp. 345-358, 2018.

[36] M. D. Lydia, K. S. Sindhu, and K. Gugan, "Analysis on solar panel crack detection using optimization techniques," *Journal of Nano-and Electronic Physics*, vol. 9, no. 2, p. 2004-1, 2017.

[37] A. H. Aghamohammadi, A. S. Prabuwono, S. Sahran, and M. Mogharrebi, "Solar cell panel crack detection using particle swarm optimization algorithm," in *2011 International Conference on Pattern Analysis and Intelligence Robotics*, vol. 1, pp. 160-164, 2011.

[38] B. Xue, F. Li, M. Song, X. Shang, D. Cui, J. Chu, and S. Dai, "Crack extraction for polycrystalline solar panels," *Energies*, vol. 14, no. 2, p. 374, 2021.

[39] A. Ennemri, P. O. Logerais, M. Balistrou, J. F. Durastanti, I. Belaidi, *et al.*, "Cracks in silicon photovoltaic modules: a review," *Journal of Optoelectronics and Advanced Materials*, vol. 21, no. 1-2, pp. 74-92, 2019.

[40] C. Chellaswamy and R. Ramesh, "An optimal parameter extraction and crack identification method for solar photovoltaic modules," *ARPN Journal of Engineering and Applied Sciences*, vol. 11, no. 24, pp. 14468-14481, 2016.

[41] S. Prabhakaran, R. Annie Uthra, and J. Preetharoselyn, "Comprehensive analysis of defect detection through image processing and machine learning for photovoltaic panels," in *Computer Vision and Machine Intelligence Paradigms for SDGs: Select Proceedings of ICRTAC-CVMIP 2021*, pp. 245-261, Springer, 2023.

[42] M. Perarasi and G. Ramadas, "Detection of cracks in solar panel images using improved AlexNet classification method," *Russian Journal of Nondestructive Testing*, vol. 59, no. 2, pp. 251-263, 2023.

[43] O. D. Singh, S. Gupta, and S. Dora, "Segmentation technique for the detection of micro-cracks in solar cells using support vector machine," *Multimedia Tools and Applications*, vol. 82, no. 21, pp. 32091-32116, 2023.

[44] W. Tang, Q. Yang, and W. Yan, "Deep learning-based algorithm for multi-type defects detection in solar cells with aerial EL images for photovoltaic plants," *CMES-Computer Modeling in Engineering & Sciences*, vol. 130, no. 3, pp. 1227-1242, 2022.

[45] S. Gundawar, N. Kumar, N. R. Meetei, G. K. Priya, S. E. Puthanveetil, and M. Sankaran, "Deep learning-based automatic micro-crack inspection in space-grade solar cells," in *Advances in Small Satellite Technologies: Proceedings of 1st International Conference on Small Satellites*, Springer, pp. 293-308, 2020.

[46] C. Mantel, F. Villebro, G. A. dos Reis Benatto, H. R. Parikh, S. Wendlandt, K. Hossain, P. Poulsen, S. Spataru, D. Sera, and S. Forchhammer, "Machine learning prediction of defect types for electroluminescence images of photovoltaic panels," in *Applications of Machine Learning*, vol. 11139, SPIE, Art. no. 1113904, 2019.

[47] T. Fan, T. Sun, X. Xie, H. Liu, and Z. Na, "Automatic micro-crack detection of polycrystalline solar cells in the industrial scene," *IEEE Access*, vol. 10, pp. 16269-16282, 2022.

[48] R. Al-Mashhadani, G. Alkawsi, Y. Baashar, A. A. Alkahtani, F. H. Nordin, W. Hashim, and T. S. Kiong, "Deep learning methods for solar fault detection and classification: a review," *Solar Cells*, vol. 11, p. 12, 2021.

[49] X. Qian, J. Li, J. Cao, Y. Wu, and W. Wang, "Micro-cracks detection of solar cells surface via combining short-term and long-term deep features," *Neural Networks*, vol. 127, pp. 132–140, 2020.

[50] D. Stromer, A. Vetter, H. C. Oezkan, C. Probst, and A. Maier, "Enhanced crack segmentation (eCS): a reference algorithm for segmenting cracks in multicrystalline silicon solar cells," *IEEE J. Photovoltaics*, vol. 9, no. 3, pp. 752–758, 2019.

[51] S. Umar, M. U. Nawaz, and M. S. Qureshi, "Deep learning approaches for crack detection in solar PV panels," *Int. J. Adv. Eng. Technol. Innov.*, vol. 1, no. 3, pp. 50–72, 2024.

[52] H. Verma, S. D. V. S. S. Varma, and P. R. Budarapu, "A machine learning-based image classification of silicon solar cells," *Int. J. Hydromechatronics*, vol. 7, no. 1, pp. 49–66, 2024.

[53] E. U. R. Mohammed, S. N. Reddy, and M. S. Waseem, "A comprehensive literature review on convolutional neural networks," *Authorea Preprints*, 2023.

[54] L. Alzubaidi, J. Zhang, A. J. Humaidi, A. Al-Dujaili, Y. Duan, O. Al-Shamma, J. Santamaría, M. A. Fadhel, M. Al-Amidie, and L. Farhan, "Review of deep learning: concepts,

CNN architectures, challenges, applications, future directions," *J. Big Data*, vol. 8, pp. 1–74, 2021.

[55] A.-I. Constantin, G. Iosif, R.-A. Chihaia, D. Marin, G. U. Abu Shehadeh, M. Karahan, B. Gerikoglu, and S. Stavrev, "Importance of preventive maintenance in solar energy systems and fault detection for solar panels based on thermal images," *Electrotehnica, Electronica, Automatica*, vol. 71, no. 1, 2023.

[56] M. P. Pyznar, "Washington, DC: US patent and trademark office," *US Patent*, vol. 3, p. 697, 2020.

[57] J. Wu, "Introduction to convolutional neural networks," *Nat. Key Lab. Novel Software Technol., Nanjing Univ., China*, vol. 5, no. 23, p. 495, 2017.

[58] K. O'Shea, "An introduction to convolutional neural networks," *arXiv preprint arXiv:1511.08458*, 2015.

[59] A. Játiva Torres *et al.*, "Assessing energy performance and management processes in solar photovoltaic plants," 2022.

[60] R. A. Marques Lameirinhas, C. P. C. V. Bernardo, J. P. N. Torres, H. I. Veiga, and P. Mendonça dos Santos, "Modelling the effect of defects and cracks in solar cells' performance using the d1MxP discrete model," *Sci. Rep.*, vol. 13, no. 1, p. 12490, 2023.

[61] Google Cloud, "Applications of artificial intelligence (AI)," *2024*. https://cloud.google.com/discover/ai-applications

[62] J. A. Tsanakas, L. Ha, and C. Buerhop, "Faults and infrared thermographic diagnosis in operating c-Si photovoltaic modules: A review of research and future challenges," *Renew. Sustain. Energy Rev.*, vol. 62, pp. 695–709, 2016.

[63] H. S. Munawar, A. W. A. Hammad, A. Haddad, C. A. P. Soares, and S. T. Waller, "Image-based crack detection methods: A review," *Infrastructures*, vol. 6, no. 8, p. 115, 2021.

[64] Z. Liu, "Road crack detection system using image segmentation algorithm," in *Proc. 2023 Int. Conf. Power, Commun., Computing and Networking Technol.*, pp. 1–6, 2023.

[65] L. Ali, F. Alnajjar, H. A. Jassmi, M. Gocho, W. Khan, and M. A. Serhani, "Performance evaluation of deep CNN-based crack detection and localization techniques for concrete structures," *Sensors*, vol. 21, no. 5, p. 1688, 2021.

[66] K. S. Bhalaji Kharthik, E. M. Onyema, S. Mallik, B. V. V. Siva Prasad, H. Qin, C. Selvi, and O. K. Sikha, "Transfer learned deep feature based crack detection using support vector machine: a comparative study," *Sci. Rep.*, vol. 14, no. 1, p. 14517, 2024.

[67] Cambridge Dictionary, "solar energy," *@CambridgeWords*, May 10, 2023. https://dictionary.cambridge.org/dictionary/english/solar-energy

[68] Encyclopedia Britannica, “Image processing | computer science,”. https://www.britannica.com/technology/image-processing

[69] A. Rosebrock, "Convolutional neural networks (CNNs) and layer types," *Accessed: Oct.*, vol. 26, 2023.

[70] Melanie, “Transfer Learning: What is it?” *Data Science Courses | DataScientest*, Sep. 21, 2023. https://datascientest.com/en/transfer-learning-what-is-it

[71] M. Tan and Q. Le, "EfficientNet: Rethinking model scaling for convolutional neural networks," in *Proc. Int. Conf. Mach. Learn.*, pp. 6105–6114, 2019.

[72] M. Dhimish, V. Holmes, B. Mehrdadi, and M. Dales, "The impact of cracks on photovoltaic power performance," *J. Sci.: Adv. Mater. Devices*, vol. 2, no. 2, pp. 199–209, 2017.

[73] Canary Media, “Chart: Solar installations set to break global, US records in 2023,”, Sep. 15, 2023. https://www.canarymedia.com/articles/solar/chart-solar-installations-set-to-break-global-us-records-in-2023

[74] R. Tang, S. Zhang, C. Ding, M. Zhu, and Y. Gao, "Artificial intelligence in intensive care medicine: bibliometric analysis," *J. Med. Internet Res.*, vol. 24, no. 11, p. e42185, 2022.

[75] Geeks for Geeks, “Top 10 branches of Artificial Intelligence,”, Jun. 28, 2024. https://www.geeksforgeeks.org/top-10-branches-of-artificial-intelligence/

[76] I. Zyout and A. Oatawneh, "Detection of PV solar panel surface defects using transfer learning of the deep convolutional neural networks," in *Proc. 2020 Adv. Sci. Eng. Technol. Int. Conf. (ASET)*, pp. 1–4, 2020.

[77] V. H. Phung and E. J. Rhee, "A high-accuracy model average ensemble of convolutional neural networks for classification of cloud image patches on small datasets," *Appl. Sci.*, vol. 9, no. 21, p. 4500, 2019.

[78] N. Sahai, “Convolutional Neural Network: Layers, Types, & More,” *Blogs & Updates on Data Science, Business Analytics, AI Machine Learning*, Jan. 08, 2024. https://www.analytixlabs.co.in/blog/convolutional-neural-network/

[79] Safety Culture, “Renewable Energy - Definition & Types,”. https://safetyculture.com/topics/renewable-energy/

[80] A. T. A. Chowdhury and M. H. Zaman, "Uses of alternative forms of sustainable energy: case of solar photovoltaic system in the rural areas of Bangladesh," *Int. J. Bus. Manag. Tomorrow*, vol. 2, no. 2, pp. 2249–9962, 2012.

[81] M. F. Akorede, "Design and performance analysis of off-grid hybrid renewable energy systems," in *Hybrid Technologies for Power Generation*, Elsevier, pp. 35–68, 2022.

[82] www.qualitymag.com, “Image Processing for Machine Vision – How Did We Get Here? | Quality Magazine,”. https://www.qualitymag.com/articles/97373-image-processing-for-machine-vision-how-did-we-get-here

[83] Slideplayer.com, “CS654: Digital Image Analysis Lecture 17: Image Enhancement”, 2015. https://slideplayer.com/slide/7500320/

[84] Guest Blog *et al.*, "The evolution and core concepts of deep learning & neural networks," *Analytics Vidhya*, vol. 6, 2016.

[85] M. M. Sukkar, D. Kumar, and J. Sindha, "Improve detection and tracking of pedestrian subclasses by pre-trained models," *J. Adv. Eng. Comput.*, vol. 6, no. 3, pp. 215–223, 2022.

[86] E. M. Gale, N. Martin, R. Blything, A. Nguyen, and J. S. Bowers, "Are there any ‘object detectors’ in the hidden layers of CNNs trained to identify objects or scenes?" *Vision Res.*, vol. 176, pp. 60–71, 2020.

[87] J. Ahmad, S. Akram, A. Jaffar, M. Rashid, and S. M. Bhatti, "Breast cancer detection using deep learning: An investigation using the DDSM dataset and a customized AlexNet and support vector machine," *IEEE Access*, 2023.

[88] F. I. Ilmawati, K. Kusrini, and T. Hidayat, "Optimizing facial expression recognition with image augmentation techniques: VGG19 approach on FERC dataset," *Sinkron: J. Penelit. Teknik Informatika*, vol. 8, no. 2, pp. 632–640, 2024.

[89] T. Kanimozhi, V. Rajeswari, R. Suguna, J. Nirmaladevi, P. Prema, B. Janani, and R. Gomathi, "RWHO: A hybrid of CNN architecture and optimization algorithm to predict basal cell carcinoma skin cancer in dermoscopic images," *The Sci. Temper*, vol. 15, no. 02, pp. 2138–2142, 2024.

[90] Wikipedia Contributors, “Transfer learning,” *Wikipedia*, Jun. 20, 2019. https://en.wikipedia.org/wiki/Transfer_learning

[91] A. Sohail, N. U. Islam, A. U. Haq, S. U. Islam, I. Shafi, and J. Park, "Fault detection and computation of power in PV cells under faulty conditions using deep-learning," *Energy Rep.*, vol. 9, pp. 4325–4336, 2023.